Localization Algorithms in a Wireless Sensor Network Using Distance and Angular Data

by

Mahsa Najibi

B.Sc., Shiraz University, 2008

Thesis Submitted in Partial Fulfillment
of the Requirements for the Degree of
Master of Applied Science

in the
School of Engineering Science
Faculty of Applied Sciences

SIMON FRASER UNIVERSITY

Summer 2013

Approval

Name: **Mahsa Najibi**

Degree: **Master of Applied Science**

Title of Thesis: ***Localization Algorithms in a Wireless Sensor Network Using Distance and Angular Data***

Examining Committee:

Chair: **Dr. Bozena Kaminska**
Professor

Dr. Rodney G. Vaughan
Senior Supervisor
Professor

Dr. Atousa Hajshirmohammadi
Co-Supervisor
Senior Lecturer

Dr. Jie Liang
Internal Examiner
Associate Professor

Date Defended: May,10, 2013

Partial Copyright Licence

Abstract

The applications of positioning in wireless sensor networks include patient monitoring, asset tracking, and intelligent transportation including air traffic control. Popular methods are: received-signal-strength (RSS); time-of-arrival (TOA); time-difference-of-arrival (TDOA); and angle-of-arrival (AOA). Estimation is based on nonlinear equations constructed from measurements and knowledge of the anchor node geometry.

In this thesis, anchor-based line-of-sight TOA and AOA are reviewed, and new techniques, namely DAOA (differential-angle-of-arrival) and hybrid TOA/DAOA are proposed for rotating laser implementation.

For the TOA approach, a nonlinear Least Square Estimator (LSE) is applied to one- and two-dimensional systems, then the equations are linearized and solved by unconstrained/constrained LSE. This LSE procedure is also used for AOA. For DAOA, all the anchors are placed on a circle in order to simplify the solution, and then LSE is used to estimate an unlocalized node. The statistical accuracy of these methods, from simulation, is presented graphically for simple read-and-use application.

Keywords: Localization algorithms; Time-of-Arrival measurement; Angle-of-Arrival measurement; Differential-Angle-of-Arrival; Hybrid TOA/DAOA; Least Squares Estimation

Dedication

To my Love, Amir,
who generously helped me and supported me
during these years of my education.

And to my beloved parents
who supported me from miles away
each and every day.

Acknowledgements

I am cordially grateful to my senior supervisor, Dr. Rodney G. Vaughan, who taught me a lot during my Master program and helped me develop the required skills to do the research and get my thesis done. He was always supportive as a father for his students and being his student was a great chance of mine. I also want to thank my supervisor, Dr. Atousa Hajshirmohammadi for all her kindly support. She accepted to be on my committee despite her busy schedule.

I would also like to thank Dr. Jie Liang for serving as my examiner, and Dr. Bozena Kaminska for her time and energy as my defence chair.

I want to thank my lovely husband, who was so patient with all my works during these years. He was the best supporter that I had during tough days and nights.

I am forever indebted to my beloved parents and brother, and my parents-in-low and sister-in law for their endless love, support, and wisdom. They encouraged me at all times and I would have never achieved my goals without them. I can never thank them enough.

I would also like to thank all my friends who gave me the energy all the time to work.

Table of Contents

List of Figures

List of Tables

List of Acronyms

WSN	Wireless sensor network
MS	Mobile station
BS	Base station
LOS	Line of sight
NLOS	Non line of sight
GPS	Global positioning system
TOA	Time-of-arrival
TDOA	Time-difference-of-arrival
AOA	Angle-of-arrival
DAOA	Differential-angle-of-arrival
RSS	Received signal strength
RSSI	Received signal strength indicator
WLS	Weighted least squares
CLS	Constrained least squares
ULS	Unconstrained least squares
WCLS	Weighted constrained least square
WULS	Weighted unconstrained least square
CRLB	Cramer-Rao lower bound
NLS	Nonlinear least squares
NLSE	Nonlinear least squares estimator
SNR	Signal-to-noise-ratio
DNR	Distance-to-noise-ratio
A^T	Transpose of matrix A
A^{-1}	Inverse of matrix A
A^o	Optimum matrix of A
σ^2	Noise variance
$\boldsymbol{C_n}$	Noise covariance matrix
$I(\boldsymbol{x})$	Fisher information matrix for parameter vector x
$\hat{\boldsymbol{x}}$	Estimate of vector x
$diag(\boldsymbol{x})$	Diagonal matrix formed from vector x
$\boldsymbol{I}_M$	$M \times M$ identity matrix

$\mathbf{1}_M$	$M \times 1$ column vector with all ones
$\mathbf{0}_M$	$M \times 1$ column vector with all zeros
$\mathbf{0}_{M \times N}$	$M \times N$ matrix with all zeros
$\odot$	Element-by-element multiplication

Chapter 1: Introduction

Estimating the physical coordinates of a mobile station (MS) or a group of sensor nodes is a fundamental problem in wireless sensor networks (WSNs) and is often called localization [1][2][7]. This problem has received significant attention in the field of wireless communications since the U.S. Federal Communications Commission (FCC) requested the accurate location of all enhanced 911 (E911) callers to be automatically determined in the United States [18]. Although the E911 service motivated the development of cellular-aided positioning in the WSN field, accurate mobile positioning information is one of the essential features for many other applications in third generation (3G) wireless systems, but this tends to use GPS data. Some of these innovative navigation and tracking applications are asset tracking, monitoring an environment in dangerous regions, controlling traffic in streets, controlling an inventory in storehouses, intelligent transport systems, patient monitoring and personnel management in rescue operations [7][9][16]. Data gathered in most of these applications require information of the sensor positions. In order to associate the data with their origin, localization algorithms can help establish the positions of the sensors [16]. Consequently, different localization algorithms have been proposed in the literature [16][9]. An accurate location technique is far from trivial, and the meaning of "accurate" in the context of location covers a wide range.

Wireless localization mostly relies on ray theory for wave propagation. Rays cannot exist by themselves, but they are a useful model for propagation effects. The bandwidth of the signal, B Hz, gives a time resolution of $\Delta T \approx {}^{1}/_{B}$ seconds, and this in term governs the distance resolution through the speed of light, i.e., $\Delta d \approx {}^{c}/_{\Delta T}$. Accurate distance resolution requires a high bandwidth. For wireless systems that use radiowaves, the wide bandwidth is a biting constraint. However, radio waves can pass, at least to some extent, through optical obstacles, such as walls. Optical systems, implemented with lasers, can get round the bandwidth constraint. Rotating lasers are

now standard instruments for precision measurement of distance and angle for using in location algorithms; but their rays cannot pass through walls, etc.

Wireless distance measurement also requires some form of time synchronization between the transmitter and receiver(s). In radio systems, the synchronization is possible using standard communications techniques, which include the communications protocol. For example, in GPS, synchronization at the receiver can take several tens of seconds, to several minutes, depending on the gain of the antenna. In GPS, the location is calculated at the receiving terminal, and the transmissions are from multiple satellites. In other systems, the device to be located transmits the location-signal and the receivers are at known locations, and their signal reception information is coordinated so that the algorithm can estimate (assuming ray theory) the location of the transmitter. This thesis does not deal with specific communications technology or specific hardware, because this itself is a specialist topic in communications. The focus here is on the algorithms used for location. In short, it is assumed that the hardware can accurately estimate the time of arrival of ray-like signals. This allows the location problem to become purely geometric, and the algorithms use noisy distance and/or angle measurements between the sensors. This is a typical approach in much of the location literature.

A large amount of research has been undertaken for the localization problem, especially for indoor positioning. In most of this literature, ultra-wideband (UWB) radio techniques can enable location algorithms to provide good absolute localization accuracy, in principle [16]. But this assumes ray theory with no ray scattering in between the sensors of the WSN. Also, for indoor situations, the device to be located, typically the transmitter, is in close proximity to, and likely surrounded by, receiving sensors whose positions are known. This configuration allows good absolute accuracy under the usual assumptions of negligible scattering. But in practice, because of the ray scattering, the relative accuracy is poor, i.e., the location error relative to the distance between the other sensors. For example, for indoor sensors whose positions are known, a typical spacing may be ten metres, and for a location accuracy requirement of one metre, the relative location accuracy is about 10%.

For outdoor sensor networks, where the sensors can be spread widely, the relative accuracy must be very high. For example, the distance between the known 3

sensors (base stations), may be 1km, and for a location accuracy of one metre, the relative accuracy of the location systems must be 0.01%. There is still no well-accepted, simple, accurate, and energy efficient approach suitable for solving the localization issue in such WSNs [16]. Accurate positioning of a mobile station (MS) from its wireless communications signals, such as cellular or other wireless sensor networks, has also been the subject of much research owing to its usefulness and the challenges of making it accurate.

Generally, large area wireless location is essentially solved with satellite navigation systems, but there is still a need for terminals that do not have satellite systems or do not have clear access to satellite signals. Even when there is clear satellite access, such as for aircraft navigation, there is often a need for back-up navigation systems. In commercial aircraft navigation, this need is a legal requirement. The most popular satellite system is GPS (Global Positioning System) [26]. For a large number of sensors in a WSN, GPS is considered too expensive since a WSN normally implies low cost terminals [17]. GPS is unreliable (unavailable, or inaccurate) in locations where there is no direct link with the satellite constellation or there is signal interference from other users of the radio spectrum [27]. The WSN alternative solution is to have a subset of sensor terminals, or *nodes*, which are aware of their own global coordinates *a priori* by using either GPS or manual configuration [2]. Such nodes are usually time-synchronized, and may be equipped with special capabilities such as directional antennas [15]. These nodes are considered as the necessary prerequisites of localization in a network, and are called beacons or anchor nodes [2]. Their known locations help to compute other individual nodes' locations, including MSs, using techniques such as lateration, and angulation or a combination of these if the distances and angles between pairs of anchors are known [17]. Techniques which are based on the precise measurement of distance to three non-collinear anchors are called trilateration. The use of more than three anchor receivers to locate a transmitter is known as multilateration. Angulation or triangulation is based on information about angles instead of distance. Here, the MS, or the unlocalized node, is the node whose location has not yet been determined. The terms *anchor* nodes and *unlocalized* nodes are used throughout this dissertation without further elaboration. It also should be mentioned that in some circumstances in which the absolute locations of the anchors are

not available, the system is called anchor-free [15]. A number of algorithms has been proposed in the literature, e.g. [25], that could locate an unknown sensor node in such a network.

The most popular methods or measurements in the literature, e.g. [7][9][16][28][32], for estimating the position of an unknown sensor are: received-signal-strength (RSS); time-of-arrival (TOA); time-difference-of-arrival (TDOA); and angle-of-arrival (AOA). The estimation is based on a set of nonlinear equations which is constructed from these measurements, with knowledge of the BS geometry. Basically, there exist two approaches for solving these nonlinear equations. One approach is to solve them using nonlinear least squares (NLS). It just requires sufficiently precise initial estimates for global convergence because the corresponding cost functions are multimodal. However, the optimum estimation performance can be obtained from this approach [7]. The second approach to solve nonlinear equations is to reorganize the nonlinear equations into a set of linear equations and then use LS or WLS. In this case, the real-time implementation is easier and global convergence is ensured [7].

Above, a ubiquitous classification has been used between indoor and outdoor situations. An alternative classification is line-of-sight (LOS) and non-LOS (NLOS) situations. This refers to an electrical line-of-sight, so that “LOS” implies Fresnel clearance for all propagation paths. LOS is often confused with meaning an optical sight path, as in a path visible to the eye. An optical sight path seldom implies that there is LOS for radio waves. However, for laser frequencies, which are indeed optical, an eyeballed sight path normally means LOS propagation. NLOS means that the multipath propagation, or ray scattering, is significant. Here, signal energy arrives at the receiver via the different paths, and usually there is no direct (LOS) path. As a consequence, the “as the crow flies” distance is hard to relate to the derived time-of-flight of signals. NLOS is often associated with indoor propagation, where walls, etc., form the multipath scatterers. NLOS is also associated with many outdoor links, where buildings, etc., similarly form scatterers. For example, a direct path is seldom found in a cellphone link, even if the cellphone is outdoors. On the other hand, in dealing with location within a single indoor space, it is possible to have a clear direct path, i.e., LOS. For radio signals, there will be reflections, or multipath, from the indoor structure as well, and this can be difficult to suppress. If optical technology, i.e., lasers, is used, then the multipath

can be more easily suppressed, and a situation of essentially pure LOS is possible. Rotating lasers are used for LOS indoor and outdoor location.

The remainder of this thesis deals with the LOS case. However, new work undertaken by the author on NLOS location estimation, has contributed to a research paper [24], but this is still under review and is not included in this thesis. The LOS is normally a bad assumption in any radio link, but laser systems get round this problem, as noted above. One application of motivating interest for this thesis is exactly this case: a large indoor environment where 2D positioning is required on the floor to within millimetres.

Similar to the traditional triangle positioning algorithms, LOS propagation from reference stations is assumed. (Most LOS algorithms are feasible for use in suburban environments with few obstacles, and these algorithms remain the basis for NLOS positioning algorithms [8][13][33].)

The geometric positioning problem is well known, and has two main steps, viz., ranging and localization. In the ranging step, for example, in the TOA approach, the distances between an unlocalized node and different anchor nodes are measured. The localizing step means computing the unlocalized node coordinates based on distance estimates [13]. Figure 1-1 illustrates these two steps of localization.

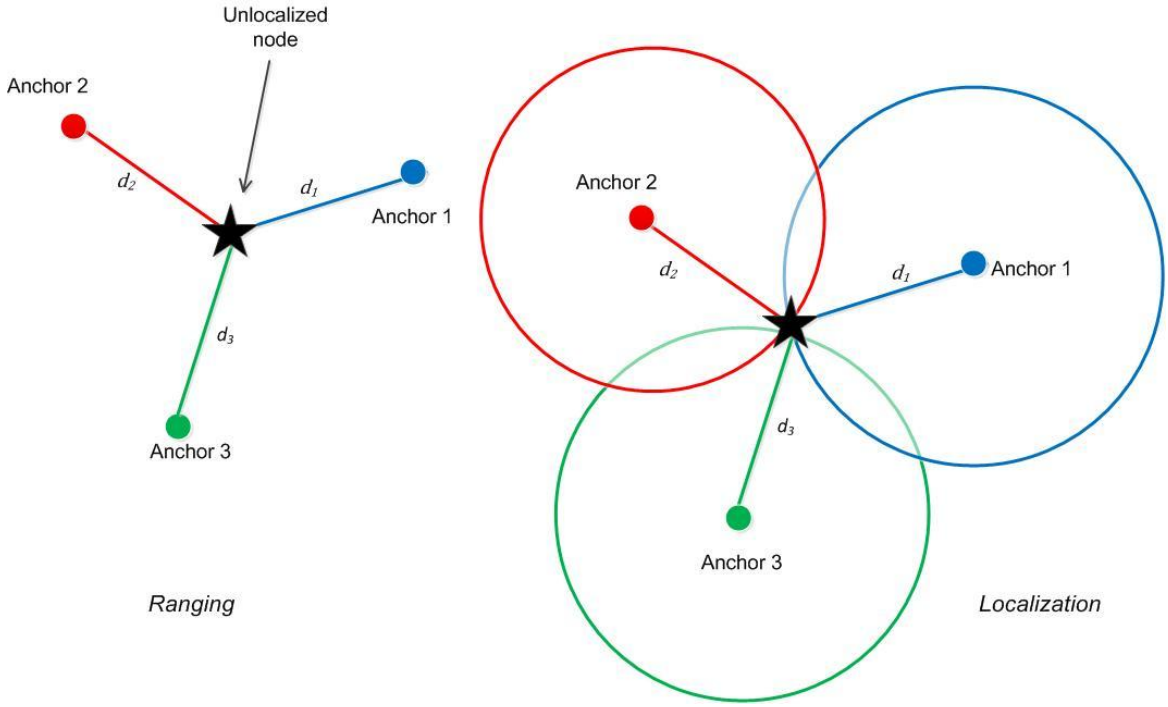

Figure 1-1. General concept of localization (adapted from [13]).

1.1. One Categorization of Sensor Network Localization Algorithms

Localization schemes can be categorized from different aspects. One category depends on the mechanism used for the localization, so in this case localization schemes can be divided into two general categories, according to [13], [21]. Normally, the localization methods are referred to as

- Range-based (uses a direct range or angle measurement of some sort.)
- Range-free (does not use a direct measurement of range or angle, etc.)

Such a broad classification restricts classification to hardware requirements of the localization schemes. The first category is based on calculating either distances or angles of the anchors with their neighbors by using technologies such as TOA, TDOA, RSS, and AOA. In the second category, only indirect distance measurements are used sometimes called proximity sensing, allows the approximate localization [21].

1.1.1. Range-Based

In this category the concept of measuring the range of wireless signal transmissions is important. Additional devices such as timers, signal strength receivers, directional antennas, and antenna arrays are used. Range-based localization relies on the availability of point-to-point distance or angle information. The obtained measurements of different ranging techniques such as TOA, TDOA, RSS, and AOA are the keys for range-based schemes for locating an unknown node [20][13]. Range-based localization will normally produce higher localization accuracy than range-free.

1.1.2. Range-Free

Range-free does not require specialist hardware to directly measure distances or angles among nodes in the system. Proximity detection (to sensors with known postions) without a range estimation, serves to coarsely locate the device [1][6][10][13][35]. This technique can be divided into two sub-categories: the local technique and the so-called hop-counting techniques [15]. In the local techniques, a node with unknown coordinates collects the proximity information of its neighbor anchor nodes with known coordinates to estimate its own coordinate. In hop-counting, each unknown node gathers the number of hops between its neighboring anchor nodes and then seeks the smallest hop count to its neighboring anchor nodes using the designated routing protocol [15]. The range-free category is included here for completeness, but is not taken further in this thesis, because it is not accurate enough.

1.2. Different Measurements of the Location Metrics

A number of methods, e.g. AOA, TOA, and RSSI (received signal strength indicator); have been published extensively for wireless positioning. In this section these most popular methods are briefly reviewed.

RSS: The RSS approach (or Signal Attenuation-Based method) attempts to calculate the mathematical model of signal path loss due to propagation [3]. This method is not pursued after this section though, because it is seldom accurate enough compared to the other methods [13]. The RSSI is a voltage at an anchor node receiver

representing the power of a known signal (a pilot for example) sent by the unlocalized node. By using at least three anchors to resolve ambiguities (in a free space type propagation model), the unlocalized node location can be estimated [13]. So, mathematically, the RSS method does not have the technical complexities of TOA or TDOA. However, any real-world radio propagation model does not give good sensitivity for mapping RSSI to range and multipath makes the situation almost impossible for reasonable accuracy [3]. It is intuitively obvious that narrowband channel RSS cannot contribute reasonable relative accuracy from standard multipath propagation considerations, and even in idealized LOS situations, an excessively high signal-to-noise ratio (SNR) - i.e., one not found in typical mobile communications – would be required for modest accuracy. Wideband RSS is also problematic, and again, an excessively high SNR would be needed to gain reasonable relative distance estimation accuracy. Finally the RSSI is the summation of all received power in the radio band of interest, so that interference – signals from other users of the spectrum – will be included. In the ISM (industrial, scientific and medical) bands, where the spectrum is unregulated, the interference would cause havoc, even in perfect LOS propagation conditions. Nevertheless, this has not stopped researchers attempting RSSI techniques for localization, perhaps because of the conceptual simplicity. The RSSI signal, corresponding to the total power in a frequency bound, is available on most receiver chips, so it does not require additional complexity. In free-space, the inverse-square law allows an estimate of the range.

The basic (without the several efficiency factors such as polarization mismatch, impedance mismatch) Friis transmission equation relates the path gain to the received power [14]:

$$P_{rec.}(d) = P_{trans.} \times G_{Tx} \times G_{Rx} \times G_{Path}\,, \qquad (1\text{-}1)$$

where d is the distance between the transmitter and the receiver. In free space, the received power–distance relationship is from the path gain (inverse of path loss) equation, $G_{path} = (4\pi d/\lambda)^{-2}$, where λ is the wavelength. For multipath situations, a reference distance, d_r, is used. By setting the reference distance to the wavelength, a

larger exponent, n_P, than for the free space path loss is applied to the excess distance, so the mean multipath gain is:

$$G_{MP} = \left(\frac{4\pi d_r}{\lambda}\right)^{-2}\left(\frac{d}{d_r}\right)^{-n_P} = (4\pi)^{-2}\left(\frac{d}{\lambda}\right)^{-n_P}. \quad (1\text{-}2)$$

The second equality follows from the choice $d_r = \lambda$ [14]. In log terms, the model of (1-1) is often expressed in a different form, as [5]

$$P_{rec.}(d) = P_r(d_r) - 10n_P\, log_{10}(\frac{d}{d_r}) + X_\sigma, \quad (1\text{-}3)$$

where $P_r(d_r)$ is the free-space power at the reference distance (between the transmitter and the receiver). In (1-3), X_σ is introduced as a statistical variation. X_σ is modelled as a zero mean log normal random variable, which represents the so-called shadow fading caused by electrically large obstacles (buildings etc.). The short-term or Rayleigh-like fading from the multipath is not explicitly in these propagation equations, although it could be included in the log normal term. So, an RSSI voltage (averaged over the short-term fading and the shadow fading), representing measurement $P_r(d)$, allows, in principle, the range to be estimated by:

$$d = d_r.\, 10^{\frac{P_r(d_r)-P_r(d)}{10n_P}}. \quad (1\text{-}4)$$

Figure 1-2 describes the distance calculation using RSS. It shows that RSS decreases proportionally to the inverse of squared distance between two nodes (for example, the unlocalized node and an anchor). So, this is the reason that RSS method does not have an accurate result for far distances even in free space.

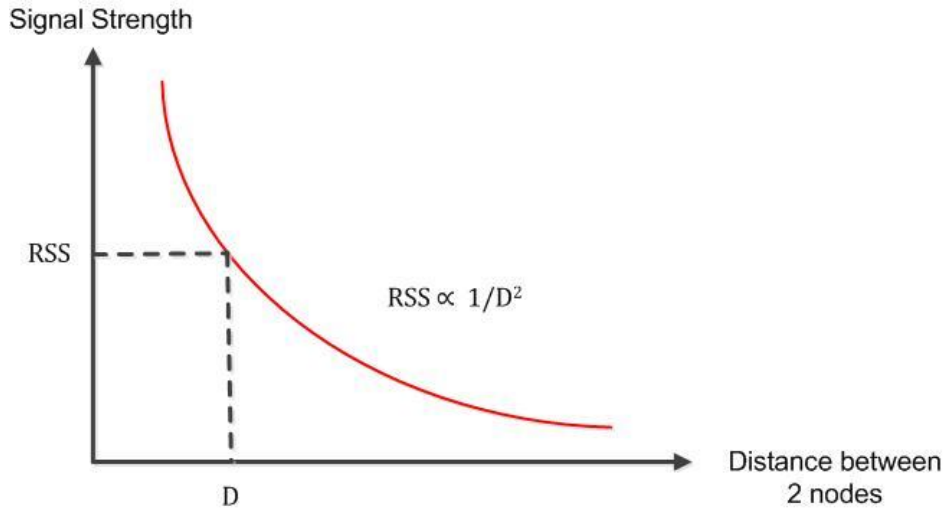

Figure 1-2. Representation scheme of RSS approach for distance estimation (adapted from [21]). D=distance between two nodes.

TOA: In the measurement of absolute TOA, the distance between the MS (or unlocalized node) and BS is taken as directly proportional to the LOS propagation time. The time is determined from the measured one-way, or sometimes two-way (c.f. radar) propagation time [7], [3]. For two-dimensional positioning, this provides a circle centered at the BS on which the MS must lie. By using at least three BSs to resolve ambiguities arising from multiple crossings of the lines of position, the MS location estimate is determined by the intersection of circles [7]. Using TOA requires that all the participating anchors and unlocalized node clocks be synchronized [13].

TDOA: The idea of TDOA is to determine the relative position of the mobile transmitter by examining the difference in time at which the signal arrives at multiple measuring units (BSs), rather than the absolute arrival time, TOA [3]. In principle, it does not require a synchronization of all the participating anchors and unlocalized node - the uncertainty between the reference time of the anchors and that of the unlocalized node can be removed by a differential calculation. Therefore, only the anchors involved in the location estimation process must be synchronized [13]. Each TDOA measurement defines a hyperbolic locus on which the MS must lie and the position estimate is given by the intersection of two or more hyperbolas [7]. So, an unknown target can be estimated in 2D plane from the two intersections of two or more TDOA measurements [3][34].

AOA: The AOA estimation method (also called Angulation Technique) requires the BSs to have multi element antenna arrays for measuring the arrival angles of the transmitted signal from the MS at the BSs. From each AOA estimate, a line of bearing (LOB) from the BS to the MS can be drawn and the position of the MS is calculated from the intersection of a minimum of two LOBs [7]. The advantages of AOA are that a position estimate may be determined with as few as three measuring units for 3D positioning or two measuring units for 2D positioning, and no time synchronization between measuring units is required.

The disadvantages include the need for relatively large and complex receiving antenna arrays and proper direction of arrival (DOA) estimation algorithms at the anchors, and location estimate degradation as the mobile target moves farther from the measuring units. For accurate positioning, the angle measurements need to be accurate. In order to get high accuracy measurements in wireless networks, influences of shadowing, multipath reflections arriving from misleading directions, or by the changing directivity of the antennas must be minimized or discarded [3]. Recently, laser techniques have enabled reliable and accurate angle measurement, and this makes AOA feasible, at least for LOS situations.

1.3. The Field of Interest and Contribution of This Thesis

As mentioned earlier, different applications of localization in wireless sensor networks make this problem scientifically interesting and many algorithms for positioning have been proposed in the literature. This thesis considers a wireless sensor network with a known number of anchors and one unlocalized node, and the whole system is static for the duration of the location estimation.

Three cases are considered. First, only noisy distances of the anchors to the unlocalized node are known. The popular TOA algorithm can be considered for this case. Second, only noisy angles subtending the anchors from the unlocalized node are known. Using the idea of AOA algorithm, a new technique, here named DAOA, is proposed. DAOA is new and has not been discussed in the literature before as far as the author is aware. Third, both noisy distances and noisy differential angles are known.

This case is similar to the popular hybrid TDOA/AOA method. However, the known angles are the angles between the anchors not the AOAs and the distances between the nodes are calculated from TOA. This latter case is feasible using laser technology, at least for LOS situations. It has not been discussed in the literature before, to the best knowledge of the author.

Besides reviewing TOA, AOA, and hybrid TDOA/AOA technique, a new contribution of this thesis is a technique which uses DAOA measurements for location estimation. The other new contribution is applying angle and distance measurements in a hybrid technique named TOA/DAOA. This latter technique turns out to perform better, but only slightly better, than TOA method. LSE is used throughout this thesis. Also, as a check, nonlinear LS is used for the estimation using TOA measurements and the results are consistent with those from unconstrained/constrained LS presented in the literature.

1.4. Summary

Geometric range-based techniques for localization using distances (distance-based) and angles measurements (angle-based) are investigated in this thesis. The first goal of this thesis is to understand and implement an estimator (algorithm) for the location in 2D where the distances (TOA) of the unknown node to known locations (anchors) are given with known statistical accuracy. As an example to fix ideas, the 2D area is square, with length 100 units. The accuracy will be expressed in these units, say metres. Since the equations obtained from the measurements are nonlinear, the first guess for the position estimation would be Nonlinear Least Squares Estimator (NLSE). The nonlinear estimators were introduced for 1D and 2D localization. Also, the unconstrained and constrained LS approach using TOA measurements is adapted from the literature. The results from the simulations for both the nonlinear and the linear unconstrained approach are consistent. So, the first goal has been attained.

A second goal is to introduce geometric localization techniques in 2D using angular measurements of the bearing to the known sensors from the unknown sensor, and specifically using differential-angle-of-arrival (DAOA) estimates. DAOA is a new technique and there are no results from the literature that can be compared to the results

presented here. It is motivated by the availability of rotating lasers which provide these measurements. The location accuracy is presented graphically, and these serve as reference performance nomograms, allowing, for example, the reader to get a feel for the number of anchors required for a given accuracy, etc. The form of these graphs seems to make sense, but they cannot be checked against existing results since no previous results have been published. The calculations are for statistical ensembles of randomly positioned anchors and unknown nodes. LS estimation is used. For DAOA, a specific system configuration that anchor nodes are on a circle around the unknown node is used. The circle configuration is not typical or realistic, but allows a simple solution using the cosine law. It offers a feel for the DAOA accuracy, even if the configuration is restricted. The formulation and solution of a general configuration for DAOA is left for future work. The second goal has therefore been partially attained. The design nomograms offer a statistically-derived feel for the performance of the new technique, and they are a new and useful contribution to this relevant location problem. However, these nomograms are restricted to the configurations that have reasonably simple solutions.

The algorithms for these new techniques are kept simple because the computation time becomes important for a dynamic situation, i.e., one where the sensors are moving, and a finite time is available to get the location estimation completed. All the location algorithms presented here all converge within a few milliseconds using a standard PC. If brute force algorithms are used, the non-linear solutions may take several minutes, and this would be too slow for most applications.

In the hybrid method, both distances and angles measurements are used together. TDOA/AOA method is reviewed briefly and the new TOA/DDAOA method is formulated. Therefore, the third goal has been attained.

Chapter 2: Localization Algorithms Using the Distances Data (TOA Measurements)

This chapter includes some geometric linear techniques for the localization of an unknown sensor node using distances measurements between that node and anchors. The new nonlinear Least Squares approaches for 1D and 2D and the Cramer-Rao-Lower-Bound for 1D are then developed. LOS propagation is assumed, following the approach of much of the literature, to establish geometric equations for position determination. In addition, TOA requires that all the participating anchors and unlocalized node clocks to be synchronized [13].

This chapter is organized as follows. Section 2.1 introduces more detail about TOA. Section 2.2 describes different estimators for a general case of using M anchors for localization. Section 2.3 presents new nonlinear algorithms using distance measurements in 1D and 2D. In section 2.4 the nonlinear equations are reorganized into a set of linear equations. So, the constrained and unconstrained Least Squares location algorithms using TOA measurements are reviewed. In order to evaluate the localization algorithm performances, simulation results are provided. Conclusions are drawn in section 2.5.

2.1. Introduction of TOA

As mentioned earlier, some nodes could be equipped with their location, e.g. through GPS [18]. These nodes become anchors, which play important roles in a wireless sensor network. One major role is aiding the location calculation of the unlocalized nodes, and the other role is to present the static coordinates of the WSN. However, some research, e.g. [31], shows the use of mobile anchors in localizing nodes can reduce the costs of hardware and deployment effort. The idea of using a mobile anchor is that more nodes get access to the anchor's signal and position, and that would

increase the location accuracy. In fact, a mobile anchor broadcasts its accurate location in the same way as a static anchor, but it represents many virtual static anchor positions. According to [19], one issue about using mobile anchors is that the anchor needs to follow the best path to maximize the improvement in location-estimation accuracy. In this thesis, the anchors are static.

In sensor networks, TOA measurements are made between each anchor and the unknown node, in order to locate the unknown node [18]. Figure 2-1 describes the distance calculation using TOA with two nodes. It shows that the distance between two nodes (for example, the unlocalized node and an anchor) is directly proportional to the one-way propagation time of the signal traveling between two nodes [3][7].

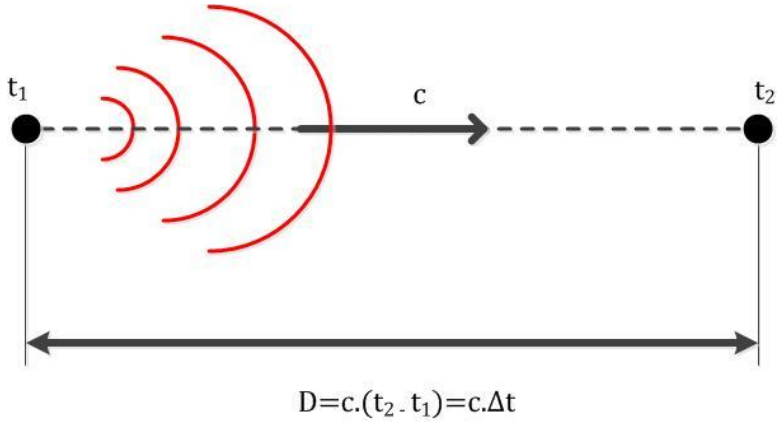

Figure 2-1. Representation scheme of TOA approach for distance estimation (adapted from [21]). D=distance between two nodes, c=signal (light) speed in free space, Δt=propagation time.

So, for M anchors (or BSs), the TOA measured at the i-th one, is (here without noise)

$$t_i = \frac{d_i}{c}, \quad i = 1,2,\dots,M, \tag{2-1}$$

where d_i is the range between the i-th BS and a node, and c is the speed of light. The time is estimated using a timer at the synchronized terminals. The synchronization is often part of existing hardware in a wireless network, with the clocks being stiff phase-locked-loops which are updated via the wireless protocol. If no such protocol exists, then the synchronization must be arranged by introducing it, and this is a difficult task.

The only alternative is to have frequency/time standards at each end of the link (such as expensive Rubidium standards). This thesis does not consider the details of the synchronization. In the presence of noise (but no multipath), the range measurement based on t_i is denoted by $r_{TOA,i}$, modeled as [29]:

$$r_{TOA,i} = d_i + n_{TOA,i} = \sqrt{(x - x_i)^2 + (y - y_i)^2} + n_{TOA,i}\,, \quad i = 1, 2, \ldots, M, \tag{2-2}$$

where $n_{TOA,i}$ is the range error in $r_{TOA,i}$, (x, y) and (x_i, y_i) are the coordinates of unlocalized node and the i-th anchor respectively. In two-dimensional (2D) positioning, the range $r_{TOA,i}$ provides a circle centered at the i-th BS on which the unlocalized node must lie. In the vector form, equation (2-2) can be expressed as [7]:

$$\boldsymbol{r}_{TOA} = \boldsymbol{f}_{TOA}(x) + \boldsymbol{n}_{TOA}\,, \tag{2-3}$$

where

$$\boldsymbol{r}_{TOA} = [r_{TOA,1}\, r_{TOA,2} \ldots r_{TOA,M}]^T\,, \tag{2-4}$$

$$\boldsymbol{n}_{TOA} = [n_{TOA,1}\, n_{TOA,2} \ldots n_{TOA,M}]^T\,, \tag{2-5}$$

$$\boldsymbol{f}_{TOA}(\boldsymbol{x}) = \begin{bmatrix} \sqrt{(x - x_1)^2 + (y - y_1)^2}) \\ \sqrt{(x - x_2)^2 + (y - y_2)^2} \\ \vdots \\ \sqrt{(x - x_M)^2 + (y - y_M)^2} \end{bmatrix}, \tag{2-6}$$

where $\boldsymbol{x} = [x \quad y]^T$.

The estimation of the unlocalized node is determined by the intersection of circles centered at the anchors. By using at least three anchors as shown in Figure 1-1, the

ambiguities arising from multiple crossings of the lines of position is resolved [7]. Section 2.1.1 also reviews a closed form algorithm for the case of using three anchors. As mentioned in the beginning of this chapter, using TOA in this thesis is based on the assumption of the synchronization of all the participating anchors and unlocalized node clocks. Now another assumption is invoked, which holds throughout this chapter, that the distances of the anchors to the unknown point are known with known statistical errors.

2.1.1. Closed Form for Two-Dimension LocalizatioUsing Three Anchors

It is recalled that the geometry of the distances using TOA measurements is a circle centered at the i-th anchor. In order to locate the unlocalized node, the circles of different anchors need to cross. At least three anchors are needed for resolving the ambiguities arising from multiple crossings of the circles. Suppose in Figure 2-2, d_1, d_2, and d_3 represent the range measurements or in other words distances between anchors to the unknown node. The geometry of these distances result in three circles passing through the unlocalized node.

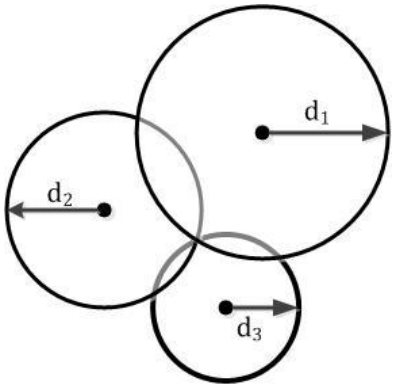

Figure 2-2. Localization of a target using three anchors (adapted from [4]).

The closed form for the location can be obtained if the following three equations solve jointly [4]:

$$d_i = \sqrt{(x_i - x)^2 + (y_i - y)^2}\,, \qquad i = 1, 2, 3; \tag{2-7}$$

where (x_i, y_i) is the known position of the i-th anchor, and (x, y) is the position of the unknown node. By solving equation (2-7), x and y can be obtained as follows

$$x = \frac{(y_2 - y_1)\gamma_1 + (y_2 - y_3)\gamma_2}{2[(x_2 - x_3)(y_2 - y_1) + (x_1 - x_2)(y_2 - y_3)]}, \quad (2\text{-}8)$$

$$y = \frac{(x_2 - x_1)\gamma_1 + (x_2 - x_3)\gamma_2}{2[(x_2 - x_1)(y_2 - y_3) + (x_2 - x_3)(y_1 - y_2)]}, \quad (2\text{-}9)$$

where

$$\gamma_1 = x_2^2 - x_3^2 + y_2^2 - y_3^2 + d_3^2 - d_2^2, \quad (2\text{-}10)$$

$$\gamma_2 = x_1^2 - x_2^2 + y_1^2 - y_2^2 + d_2^2 - d_1^2. \quad (2\text{-}11)$$

For the problem addressed in this thesis, d_1, d_2, and d_3 are known and they are not dependent on the position of the unknown point. Therefore, equations (2-8) and (2-9) can be considered as the closed form for the unlocalized node [4]. For a general case of having M anchors, an estimator should be used to localize the unknown node.

2.2. Estimators for Localization Using Different Measurement Techniques

The general idea for an estimator in the range-based schemes, for example, for using TOA is [18]:

$$\widehat{\boldsymbol{\theta}} = arg\,min_{\boldsymbol{\theta}} \sum_{i \in M} \rho(r_i - \|\boldsymbol{\theta} - \boldsymbol{k}_i\|); \; i = 1,2,\ldots,M, \quad (2\text{-}12)$$

where $\boldsymbol{\theta} = [x, y]^T$ and $\boldsymbol{k}_i = [x_i, y_i]^T$ are the coordinates of the unknown and the i-th anchor nodes respectively. M is the total number of the anchors or the BSs. $\widehat{\boldsymbol{\theta}}$ is the

estimation of the $\boldsymbol{\theta}$ and $\|\boldsymbol{\theta} - \boldsymbol{k}_i\|$ denotes the norm operation over a vector which is the distance between the unknown node and an anchor. r_i is the noisy range measurement from the unlocalized node to i-th anchor. According to [18], $r_i - \|\boldsymbol{\theta} - \boldsymbol{k}_i\|$ is called the i-th residual for a particular $\boldsymbol{\theta}$. $\rho(.)$ is the objective (cost) function. For different criteria, different estimators can be used in order to minimize this cost function. For example, when the posterior conditional probability density function (PDF) of the location, given the measurement ($f_\theta(\boldsymbol{\theta}|\boldsymbol{r})$) is known, the minimum mean square error (MMSE) estimator is used ($\boldsymbol{\theta}$ is a random variable):

$$\widehat{\boldsymbol{\theta}}_{MMSE} = E\{\boldsymbol{\theta}|\boldsymbol{r}\} = \int_S \boldsymbol{\theta}\, f_\theta(\boldsymbol{\theta}|\boldsymbol{r})\, d\theta\,, \tag{2-13}$$

where vector $\boldsymbol{r}$ is the range measurement and S is the region in which the unknown node would reside, in other words it corresponds to all the possible values of $\boldsymbol{\theta}$ [18].

Using a maximum likelihood estimator (MLE) without *a priori* information about the distribution of the range or range difference measurements in (2-12), a probability model for (2-12) can be considered. $\hat{\theta}_{MLE}$ is an estimation of location which is calculated as [18]:

$$\widehat{\boldsymbol{\theta}}_{MLE} = arg\ max_\theta\, f_{\boldsymbol{r}}(\boldsymbol{r}|\boldsymbol{\theta})\,, \tag{2-14}$$

where $f_{\boldsymbol{r}}(\boldsymbol{r}|\boldsymbol{\theta})$ is the conditional probability density function (PDF) of the measurements given the location $\boldsymbol{\theta}$.

Taking the residual as Gaussian for simplicity, MLE has a similar result as the least square (LS) estimator which can solve $\rho(.)$ for the optimal solution. In addition, there is still no need for *a priori* information about the distribution of the range or range difference measurements in (2-12) [18].

Examples of other proposed localization algorithms include Bayesian techniques and Kalman filtering, but since LSE is a common and reliable technique for the current case study, it is used throughout this thesis.

2.3. Nonlinear Localization Algorithms Using Distance Measurements

2.3.1. Localization in One-Dimension Using Nonlinear Least Squares Estimator

In order to estimate the position of the unknown node from a set of nonlinear equations featuring the TOA measurements, more attention is now directed to minimizing the sum of squares of nonlinear equations. One of the approaches to tackle this problem is the least-squares algorithm [3]. Below, the estimation of the unlocalized node is proposed to be undertaken using nonlinear least squares (NLS). For simplification the procedure is applied to the one-dimensional case first and then TO the two-dimensional case.

Procedure

The noisy distance between two points in 2D coordinates is:

$$(x - x_i)^2 + (y - y_i)^2 = d_i^2 + n_i \qquad (2\text{-}15)$$

where (x, y) and (x_i, y_i) are the location of unknown node and i-th anchor respectively, d_i is the distance between them and n_i is the additive Gaussian noise. So, the one-dimensional topology is that all the anchors and the unknown node are on a straight line. It is assumed that the distances between the known points (anchors) and the unknown one are measurements. In one-dimensional case, the noise is:

$$n_i = (x - x_i)^2 - d_i^2 \ . \qquad (2\text{-}16)$$

The Least Squares Estimation can be used to estimate the unknown node in the following form:

$$\hat{x}_{NLS} = arg\,min_x\ J;\ J = \sum_{i=1}^{M}[(x - x_i)^2 - d_i^2]^2 \qquad (2\text{-}17)$$

The expansion of J can be found in Appendix A (see (A.1)-(A.6)). In order to minimize J, its derivative with respect to x (see (A.7)) should be set to zero. The calculation ends up with a cubic equation of x which has one real root. The solution of this root is used for the simulation:

$$x = -\frac{b}{3a} - \frac{2^{1/3}\,(-b^2 + 3ac)}{3au} + \frac{u}{3 \times 2^{1/3} a}\ ; \qquad (2\text{-}18)$$

where u is:

$$(\ -2b^3 + 9abc - 27a^2d + \sqrt{4(-b^2 + 3ac)^3 + \ (-2b^3 + 9abc - 27a^2d)^2}\ )^{1/3}\ . \qquad (2\text{-}19)$$

The parameters of (2-18) and (2-19) are defined in Table 2-1. ((A.8) and (A.9) show x and u with the substituted parameters.)

It is obvious that if the system was noiseless, the estimated result would be the exact position of the unknown node. Now noise is added, and it is taken as zero-mean Gaussian with variance of σ^2 because of convenience rather than any underlying physical mechanism. A closed form geometric solution could be obtained for the one-dimensional case. However, the cubic equation makes it hard to calculate the expectation of error for evaluating the performance of the estimator. Therefore the Cramér–Rao Lower Bound (CRLB) is derived as a benchmark of the location accuracy. It provides a lower bound on the variance of the unbiased estimator with which the algorithms can be compared [9]. The Cramér–Rao lower bound has the lowest possible mean squared error and there is no lower error variance among all unbiased methods. Appendix B provides the details on the derived CRLB for the one-dimensional case of the problem.

Table 2-1. Definitions of the parameters in equations (2-18) and (2-19)

Parameter	Definition
a	M : Number of anchors
b	$-3\ \mathbf{1}_M^T\ \boldsymbol{v}$: where $\boldsymbol{v} = \begin{bmatrix} x_1 \\ \vdots \\ x_M \end{bmatrix}$; x_{i} is the x coordinate of i-th anchor.
c	$2\ \boldsymbol{v}^T\ \boldsymbol{v}\ + \mathbf{1}_{\boldsymbol{M}}^T\ \boldsymbol{p} - D^T D$: $\boldsymbol{v}$ is the same as above, $\boldsymbol{p} = \begin{bmatrix} x_1^2 \\ \vdots \\ x_M^2 \end{bmatrix}$, and $D = \begin{bmatrix} d_1 \\ \vdots \\ d_M \end{bmatrix}$; d_{i} is the distance of i-th anchor to the unknown node.
d	$D^T(\boldsymbol{v}\ \odot\ D) - \boldsymbol{p}^T\ \boldsymbol{v}$: $\boldsymbol{v}$, $\boldsymbol{p}$ and D are the same as above and $\odot$ is an element-by-element multiplication operator.

Simulation Results

The Mean Square Error (MSE) is used to study the estimator's accuracy. Figure 2-3 shows the decreasing MSE with increasing number of anchors from 4 to 20. (The MSE for 3 anchors is also calculated and it is 0.057.) For the simulation, the anchors are placed randomly along 100 units line. The number of realizations for the estimation is 10^4 and the Gaussian noise variance is 0.1. According to the derived formula (see Appendix) for the CRLB in 1D, $(\frac{\sigma^2}{M})$, the number of anchors and the noise variance are important for the CRLB. The distance between the empirical curve and the CRLB gives the performance of the estimator.

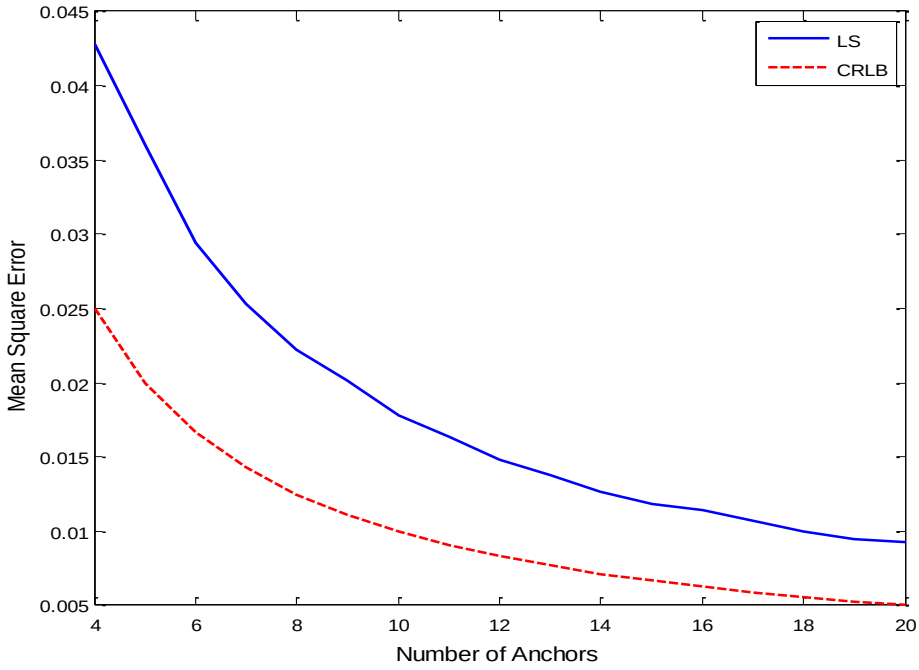

Figure 2-3. Mean square error vs. number of anchors in 1D using nonlinear LS estimator.

For example, for 10 anchors, MSE is around 0.018 and 0.01, for the empirical LS and the CRLB, respectively. It is also shown that for using more anchors, the performance of the estimator would be closer to the CRLB.

Another way to study the accuracy is the comparison of MSE versus SNR (signal-to–noise-ratio). A distance-to-noise-ratio (DNR) is introduced here which is the ratio between the squared mean of the distance, u_d^2, and the noise variance σ_n^2. So, DNR is calculated from $10\log\frac{u_d^2}{\sigma_n^2}$. Figure 2-4 shows the MSE versus DNR (dB) in one-dimensional case for 10 and 20 anchors and variance noise of 0.1 to 10. The figure gives a feel for the accuracy. For example, for $DNR = 25\ dB$, if 10 anchors are used, the MSE is 0.5. Similarly if an accuracy of 0.3% is required, then for 20 anchors, DNR must be about 24. Note that the "range noise" variance, σ_n^2, does not depend on the distance (range), so physically its value is governed by the receiver noise process, and not a decrease of range sensing signal strength.

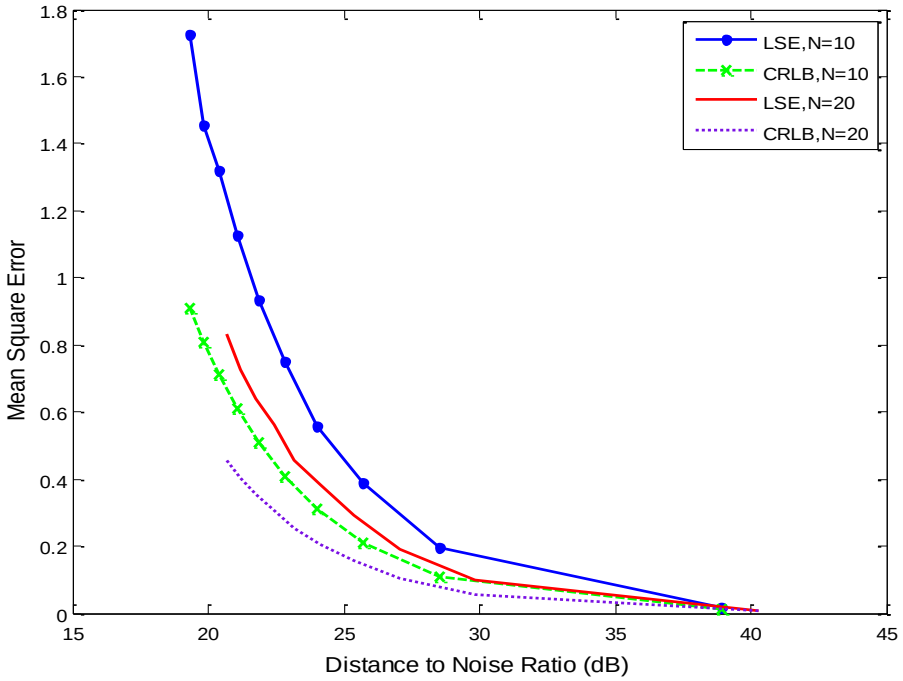

Figure 2-4. Mean square error vs. DNR (dB) in 1D using nonlinear LS estimator. The "Distance" is from the squared mean distance between the unlocalized node and the anchors averaged over an ensemble of 10^4 uniformly anchors distributions along a 100 units line.

Comparing the estimator performance to the CRLB reveals that by decreasing the noise variance, the empirical curve becomes closer to the CRLB.

2.3.2. Localization in Two Dimensions Using NLSE

In the 2D case, all the anchors and the unknown node are in the $x-y$ plane. All the steps mentioned for the one-dimensional localization can be repeated for the proposed two-dimensional case using nonlinear LS as well. Again, the noisy distances between the node to be located, and the anchors, are the observations. The only difference of the 2D case with the 1D is that now there are two cubic equations after taking derivatives of J with respect to x and y.

Procedure

Consider $\boldsymbol{\theta}$ as the coordinates of the unknown node ($\boldsymbol{\theta} = [x, y]^T$), the cost function (J) for 2D becomes:

$$\widehat{\boldsymbol{\theta}} = arg\,min_{\boldsymbol{\theta}}\, J \;;\; J = \sum_{i}^{M} \left[(x - x_i)^2 + (y - y_i)^2 - d_i^2\right]^2. \tag{2-20}$$

After some vector calculations (details can be found on (A.10)-(A-14) in Appendix A), the derivations with respect to x and y are derived (see (A-15)-(A-18) for details). Then x and y can be obtained by finding the roots of the following two simultaneous equations:

$$y^2\,(Mx - \mathbf{1}_M^T \boldsymbol{v}) + y\,(\mathbf{1}_M^T\,(\boldsymbol{v} \odot \boldsymbol{w}) - 2x\,\mathbf{1}_M^T\,\boldsymbol{w} + \boldsymbol{w}^T\,\boldsymbol{v}) + \boldsymbol{f}(x) = 0\,; \tag{2-21}$$

$$x^2\,(My - \mathbf{1}_M^T \boldsymbol{w}) + x\,(\mathbf{1}_M^T\,(\boldsymbol{v} \odot \boldsymbol{w}) - 2y\,\mathbf{1}_M^T\,\boldsymbol{v} + \boldsymbol{w}^T\,\boldsymbol{v}) + \boldsymbol{g}(y) = 0\,; \tag{2-22}$$

where $\boldsymbol{f}(x)$ and $\boldsymbol{g}(y)$ are:

$$\boldsymbol{f}(x) = Mx^3 - 3x^2\mathbf{1}_M^T\boldsymbol{v} + x\,(2\boldsymbol{v}^T\boldsymbol{v} + 1^T\boldsymbol{p} + \boldsymbol{w}^T\boldsymbol{w} - D^TD) - \boldsymbol{p}^T\boldsymbol{v} - \boldsymbol{w}^T(\boldsymbol{v} \odot \boldsymbol{w}) + D^T(D \odot \boldsymbol{v}); \tag{2-23}$$

$$\boldsymbol{g}(y) = My^3 - 3y^2\mathbf{1}_M^T\boldsymbol{w} + y(2\boldsymbol{w}^T\boldsymbol{w} + \mathbf{1}_M^T\boldsymbol{q} + \boldsymbol{v}^T\boldsymbol{v} - D^TD) - \boldsymbol{q}^T\boldsymbol{w} - \boldsymbol{v}^T(\boldsymbol{v} \odot \boldsymbol{w}) + D^T(D \odot \boldsymbol{w}); \tag{2-24}$$

where x and y are the position of the target or unknown node. Other parameters are the same as defined in Table 2-1. In addition $\boldsymbol{w}$ is a column vector consists of y coordinates of the anchors ($\boldsymbol{w} = \begin{bmatrix} y_1 \\ \vdots \\ y_M \end{bmatrix}$).

Apparently there is no closed form solution for the 2D equations (2.21) and (2.22). Numerical solution is required, and standard MTLAB routines are used here to solve both equations simultaneously.

Simulation Results

For each observation in the simulations, the anchors are located uniformly in $x - y$ plane in a 100 by 100 square area. For example, Figure 2-5 shows one realization of 10 anchors and the unlocalized node. A random constellation of anchors is considered with random noises for the distances, in each simulation run.

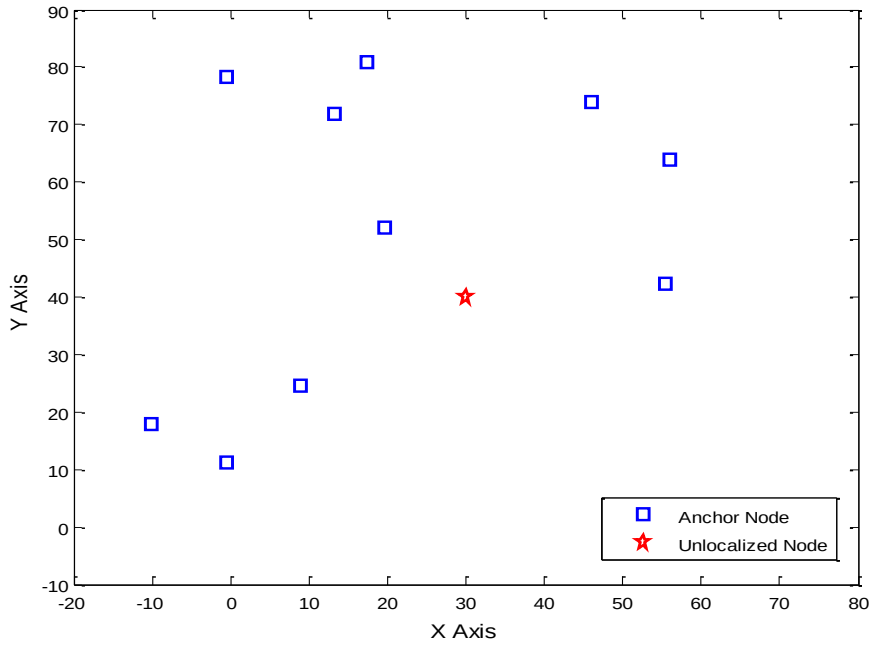

Figure 2-5. One realization of 10 anchors and the unlocalized node in a 100 by 100 square area.

Figure 2-6 shows the performance of the estimator (i.e., the numeric solution above) for 2D by applying different number of anchors from 4 to 20 anchors for 10^4 observations. (The MSE for 3 anchors is also calculated to be 0.49.)

For each observation, the anchors are uniformly distributed in a 100 by 100 square and the Gaussian noise variance is 0.1.

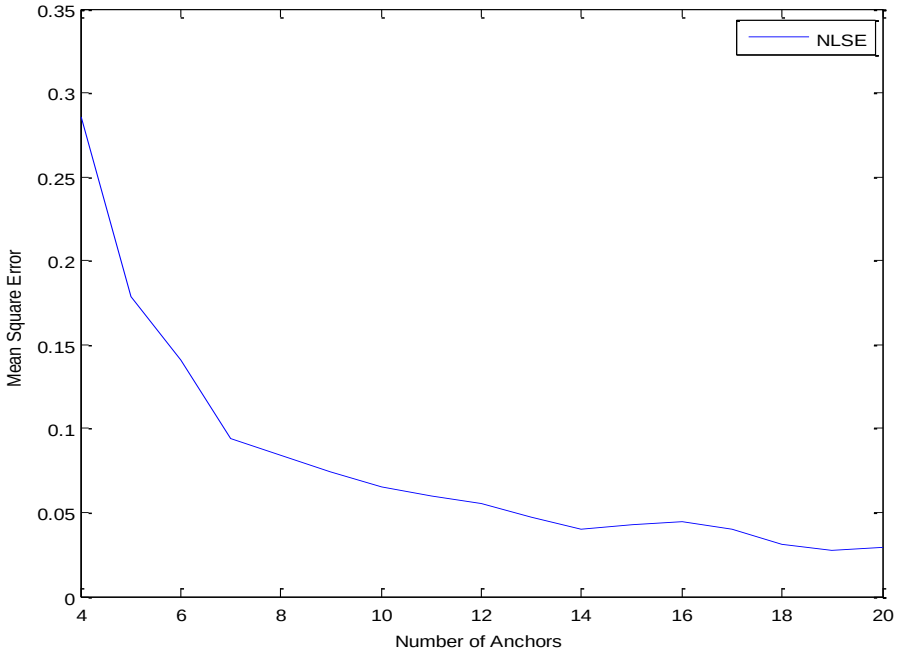

Figure 2-6. Mean square error vs. number of anchors in 2D using nonlinear LS estimator. Noise variance is 0.1, and DNR=41 dB.

The figure shows that using more than about 10 anchors sees diminishing returns for the location accuracy. As sample tie-points, 4 anchors give an MSE of 0.28, and 7 anchors give an MSE of less than 0.1. (10 anchors give MSE about 0.07, and 20 give 0.03.)

As mentioned earlier, another way to view the accuracy is to plot MSE versus DNR (dB). The result is shown in Figure 2-7 for 10^4 observations and the noise variance varies from 0.1 to 10. For the same DNR, the estimator using 20 anchors has a lower MSE.

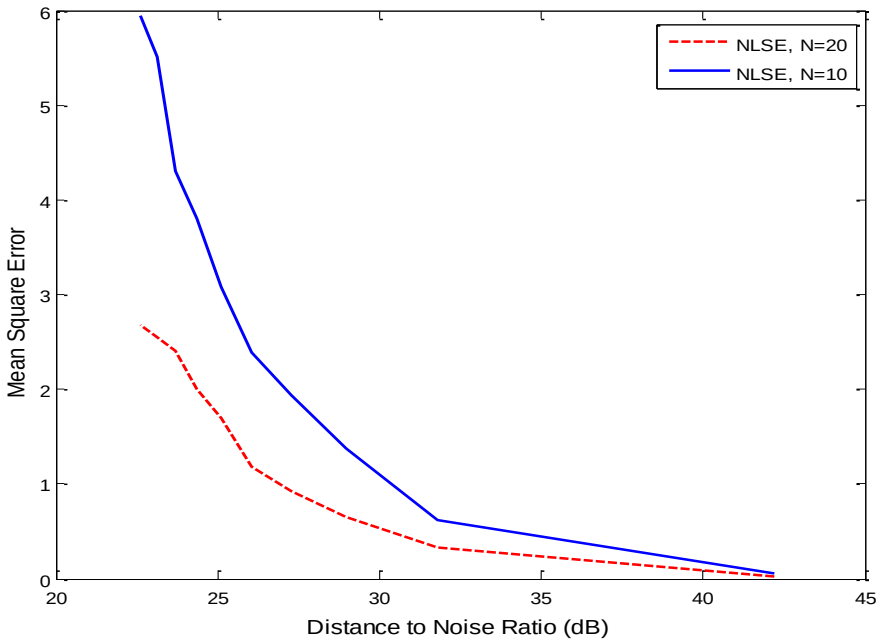

Figure 2-7. Mean square error vs. DNR (db) in 2D using nonlinear LS estimator. The "Distance" is from the squared mean distance between the unlocalized node and the anchors averaged over an ensemble of 10^4 uniformly anchors distributions in a 100 by 100 square.

The range of MSE in 2D case is larger than MSE range in 1D, because there are noises in both x and y directions. By increasing DNR to around 41 MSE decreases to zero. This point corresponds to the lowest amount of noise variance which is 0.1.

The reason is that the approach in much of the literature is to work with linear formulations. This is perhaps because these are faster in implementation and simulation. A nonlinear estimator could not be found by the author for comparison with the nonlinear LS estimator proposed in this thesis.

2.4. An Unconstrained/Constrained Least Squares Approach for Positioning Using TOA Measurement

In this section the nonlinear equations are reorganized into a set of linear equations and then the LS estimator is used. The development of unconstrained and constrained LS location algorithms using TOA measurements in this section (2.4) is

adapted from [29]. The distance between the unlocalized node and the i-th anchor is denoted by $r_{TOA,i}$ from equation (2-2), and without considering the noise, this would be:

$$\boldsymbol{r}_{TOA,i} = [(x - x_i)^2 + (y - y_i)^2]^{\frac{1}{2}}, \qquad i = 1, 2, \dots, M. \tag{2-25}$$

Recalling that (x, y) is the position of the unlocalized node and the known coordinates of the i-th anchor is (x_i, y_i).

2.4.1. Algorithm Development

Squaring both sides of (2-25) yields [29]:

$$\boldsymbol{r}_{TOA,i}^2 = (x^2 + y^2) - 2xx_i - 2yy_i + \left(x_i^2 + y_i^2\right). \tag{2-26}$$

An intermediate variable, R, is used here to linearize (2-26) in terms of x, y and R^2 [29].

$$R = \sqrt{x^2 + y^2} \tag{2-27}$$

It is clear that R is the distance between (x, y) and the reference origin. So, by using this intermediate variable, (2-26) will change to:

$$xx_i + yy_i - 0.5\, R^2 = \frac{1}{2}\left(x_i^2 + y_i^2 - \boldsymbol{r}_{TOA,i}^2\right), \quad i = 1, 2, \dots, M. \tag{2-28}$$

(2-28) can be represented in matrix-vector form as:

$$\boldsymbol{A\theta} = \boldsymbol{b}, \tag{2-29}$$

where

$$\boldsymbol{A} = \begin{bmatrix} x_1 & y_1 & -0.5 \\ \vdots & \vdots & \vdots \\ x_M & y_M & -0.5 \end{bmatrix}, \quad \boldsymbol{\theta} = \begin{bmatrix} x \\ y \\ R^2 \end{bmatrix}, \quad \boldsymbol{b} = \frac{1}{2} \begin{bmatrix} x_1^2 + y_1^2 - r_{TOA,1}^2 \\ \vdots \\ x_M^2 + y_M^2 - r_{TOA,M}^2 \end{bmatrix}. \tag{2-30}$$

Since the third element of $\boldsymbol{\theta}$, R^2, is the function of the first two elements, so $\boldsymbol{\theta}$ should be estimated by Constrained Least Squares (CLS) (which is suggested by [29] and will be discussed later in this section). However, if R is considered as an unknown parameter, for the linear model $\boldsymbol{A\theta} = \boldsymbol{b}$, $\boldsymbol{\theta}$ can be estimated (unconstrained) as:

$$\widehat{\boldsymbol{\theta}} = (\boldsymbol{A}^T \boldsymbol{A})^{-1} \boldsymbol{A}^T \boldsymbol{b}. \tag{2-31}$$

where the cost function is [29]:

$$J = (\boldsymbol{A\theta} - \boldsymbol{b})^T (\boldsymbol{A\theta} - \boldsymbol{b}), \tag{2-32}$$

The simulation results for this unconstrained approach are shown in Figure 2-8 and Figure 2-9. In general, the CLS estimate of $\boldsymbol{\theta}$ is obtained by minimizing the cost function subject to the following constraint in (2-33). The constraint is a matrix characterization of the relation in (2-27):

$$\boldsymbol{q}^T \boldsymbol{\theta} + \boldsymbol{\theta}^T \boldsymbol{P} \boldsymbol{\theta} = \boldsymbol{0}, \tag{2-33}$$

such that

$$\boldsymbol{P} = \begin{bmatrix} 1 & 0 & 0 \\ 0 & 1 & 0 \\ 0 & 0 & 0 \end{bmatrix}, \quad \boldsymbol{q} = \begin{bmatrix} 0 \\ 0 \\ -1 \end{bmatrix}. \tag{2-34}$$

Now the method of Lagrange multipliers is used to minimize a function subject to a constraint. The cost function is

$$J = \boldsymbol{\theta}^T \boldsymbol{A}^T \boldsymbol{A}\boldsymbol{\theta} + \boldsymbol{b}^T \boldsymbol{b} - 2\boldsymbol{\theta}^T \boldsymbol{A}^T \boldsymbol{b} + \boldsymbol{\lambda}\,(\boldsymbol{q}^T \boldsymbol{\theta} + \boldsymbol{\theta}^T \boldsymbol{P}\,\boldsymbol{\theta})\,, \tag{2-35}$$

where $\boldsymbol{\lambda}$ is the corresponding Lagrange multiplier. In order to minimize J, its derivative with respect to $\boldsymbol{\theta}$ is taken,

$$\frac{\partial J}{\partial \boldsymbol{\theta}} = 2\boldsymbol{A}^T \boldsymbol{A}\boldsymbol{\theta} - 2\,\boldsymbol{A}^T \boldsymbol{b} + \boldsymbol{\lambda}\,(\boldsymbol{q} + 2\boldsymbol{P}\boldsymbol{\theta}) = 0\,, \tag{2-36}$$

and its root should be found which leads to:

$$(2\boldsymbol{A}^T \boldsymbol{A} + 2\boldsymbol{\lambda}\boldsymbol{P})\boldsymbol{\theta} = 2\boldsymbol{A}^T \boldsymbol{b} - \boldsymbol{\lambda}\boldsymbol{q}\,. \tag{2-37}$$

So, the constrained estimated of $\boldsymbol{\theta}$ is:

$$\widehat{\boldsymbol{\theta}} = (2\boldsymbol{A}^T \boldsymbol{A} + 2\boldsymbol{\lambda}\boldsymbol{P})^{-1}(2\boldsymbol{A}^T \boldsymbol{b} - \boldsymbol{\lambda}\boldsymbol{q})\,. \tag{2-38}$$

The parameter $\boldsymbol{\lambda}$ is still unknown in the $\widehat{\boldsymbol{\theta}}$. So, (2-38) is substituted into (2-33):

$$\begin{aligned} &\boldsymbol{q}^T\,(2\boldsymbol{A}^T \boldsymbol{A} + 2\boldsymbol{\lambda}\boldsymbol{P})^{-1}(2\boldsymbol{A}^T \boldsymbol{b} - \boldsymbol{\lambda}\boldsymbol{q}) + \\ &(2\boldsymbol{A}^T \boldsymbol{b} - \boldsymbol{\lambda}\boldsymbol{q})^T(2\boldsymbol{A}^T \boldsymbol{A} + 2\boldsymbol{\lambda}\boldsymbol{P})^{-1}\,\boldsymbol{P}\,(2\boldsymbol{A}^T \boldsymbol{A} + 2\boldsymbol{\lambda}\boldsymbol{P})^{-1}(2\boldsymbol{A}^T \boldsymbol{b} - \boldsymbol{\lambda}\boldsymbol{q}) = 0. \end{aligned} \tag{2-39}$$

$\boldsymbol{\lambda}$ can be determined numerically from equation (2-39) and then it is substituted in (2-38) in order to find $\widehat{\boldsymbol{\theta}}$.

So far all the elements of the minimization algorithm in the LS estimator are considered with the same weight. In some literature, e.g. [29], a weighting matrix is used

to get a better performance. The estimates of $\boldsymbol{\theta}$ based on the WULS (weighted unconstrained least squares) are obtained by:

$$\widehat{\boldsymbol{\theta}} = (\boldsymbol{A}^T \boldsymbol{\Psi}^{-1} \boldsymbol{A})^{-1} (\boldsymbol{A}^T \boldsymbol{\Psi}^{-1} \boldsymbol{b}). \tag{2-40}$$

where the weighted cost function is [29]:

$$J = (\boldsymbol{A\theta} - \boldsymbol{b})^T \boldsymbol{\Psi}^{-1} (\boldsymbol{A\theta} - \boldsymbol{b}) , \tag{2-41}$$

For the WCLS (weighted constrained leas squares), the estimates of $\boldsymbol{\theta}$ are computed by minimizing the (2-41) subject to (2-33). In fact (2-40) and (2-41) are similar to (2-31) and (2-32) respectively with $\boldsymbol{\Psi}^{-1}$ as their corresponding weighting matrix. According to [7] the optimum value of this weighting matrix is determined based on the BLUE (best linear unbiased estimator) as follows. For sufficiently small measurement errors, the value of $\boldsymbol{r}_{TOA,i}^2$ in (2-15) can be approximated as

$$\boldsymbol{r}_{TOA,i}^2 = (d_i + n_{TOA,i})^2 \approx d_i^2 + 2 (d_i)^2 n_{TOA,i} , \qquad i = 1, 2, \dots, M . \tag{2-42}$$

The difference between the estimate of the squared distances and the true value squared is defined as the *disturbance* [7] (same as the error energy):

$$\varepsilon_i = r_{TOA,i}^2 - d_i^2 \approx 2 d_i n_{TOA,i} , \qquad i = 1, 2, \dots, M . \tag{2-43}$$

In vector form, $\{\varepsilon_i\}$ is expressed as

$$\boldsymbol{\varepsilon} = [2 d_1 n_{TOA,1} , 2 d_2 n_{TOA,2} , \dots, 2 d_M n_{TOA,M}]^T. \tag{2-44}$$

The optimum weighting matrix uses the covariance matrix of the disturbance in the form of

$$\Psi^0 = E\{\boldsymbol{\varepsilon}\boldsymbol{\varepsilon}^T\} = \boldsymbol{s}\,\boldsymbol{s}^T \odot \boldsymbol{C}_{\boldsymbol{n},TOA}\ , \tag{2-45}$$

where

$$\boldsymbol{s} = [\ d_1\ \ d_2\ \ \ldots\ \ d_M]^T\ , \tag{2-46}$$

where the distances $\{d_i\}$ are known. Since all the measurement errors are considered uncorrelated, the covariance matrix of that would be a diagonal matrix:

$$\boldsymbol{C}_{\boldsymbol{n},TOA} = \begin{bmatrix} \sigma_{TOA,1}^2 & 0 & \ldots & 0 \\ 0 & \sigma_{TOA,2}^2 & \ldots & 0 \\ \vdots & \vdots & \ddots & \vdots \\ 0 & 0 & \ldots & \sigma_{TOA,M}^2 \end{bmatrix}. \tag{2-47}$$

So, the ideal weighting matrix for the TOA-based algorithm is:

$$\boldsymbol{\Psi} \approx \boldsymbol{s}\boldsymbol{s}^T \odot \boldsymbol{C}_{\boldsymbol{n},TOA} = \begin{bmatrix} d_1^2\sigma_{TOA,1}^2 & 0 & \ldots & 0 \\ 0 & d_2^2\sigma_{TOA,2}^2 & \ldots & 0 \\ \vdots & \vdots & \ddots & \vdots \\ 0 & 0 & \ldots & d_M^2\sigma_{TOA,M}^2 \end{bmatrix}. \tag{2-48}$$

Considering (2-35) and (2-38) with the corresponding weighting matrix:

$$J = \boldsymbol{\theta}^T\boldsymbol{A}^T\boldsymbol{\Psi}^{-1}\boldsymbol{A}\boldsymbol{\theta} + \boldsymbol{b}^T\boldsymbol{\Psi}^{-1}\boldsymbol{b} - 2\boldsymbol{\theta}^T\boldsymbol{A}^T\boldsymbol{\Psi}^{-1}\boldsymbol{b} + \boldsymbol{\lambda}\,(\boldsymbol{q}^T\boldsymbol{\theta} + \boldsymbol{\theta}^T\boldsymbol{P}\boldsymbol{\theta}), \tag{2-49}$$

$$\widehat{\boldsymbol{\theta}} = (2\boldsymbol{A}^{\boldsymbol{T}}\boldsymbol{\Psi}^{-1}\boldsymbol{A} + 2\boldsymbol{\lambda}\boldsymbol{P})^{-1}\left(2\boldsymbol{A}^{\boldsymbol{T}}\boldsymbol{\Psi}^{-1}\boldsymbol{b} - \boldsymbol{\lambda}\boldsymbol{q}\right), \tag{2-50}$$

where $\boldsymbol{\lambda}$ is the corresponding Lagrange multiplier and can be determined from the equation of (2-39).

Simulation Results

In this section the simulation results of the algorithms are provided. Figure 2-8 presents the performances of the unconstrained, weighted unconstrained and constrained least square estimators for different number of anchors from 4 to 20. (The MSE for 3 anchors is also calculated for ULS, WULS, and CLS which are 6.37, 5.41, and 0.51 respectively.)

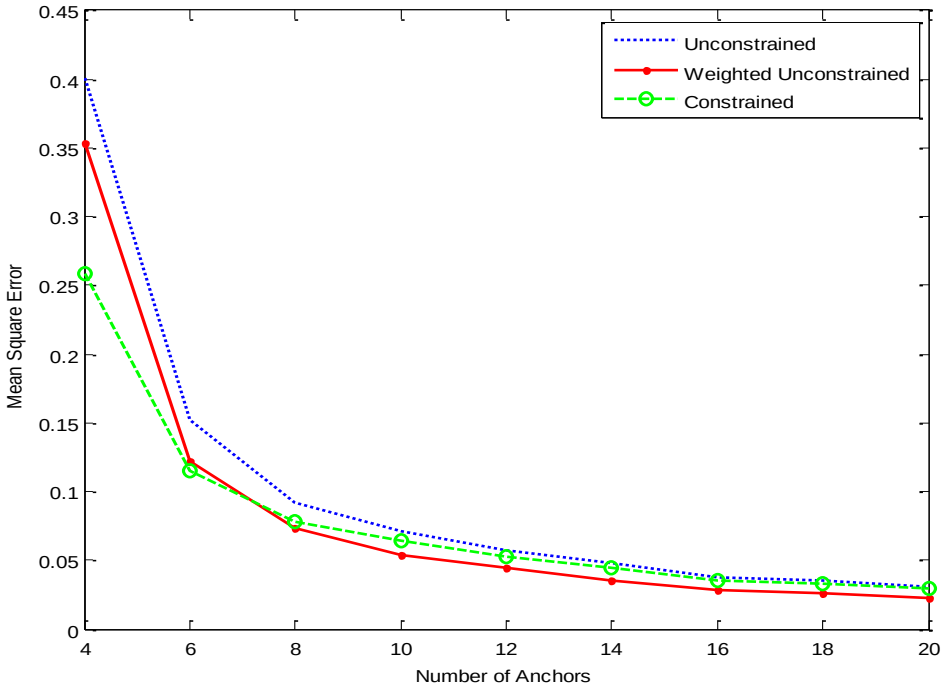

Figure 2-8. MSE vs. number of anchors in 2D using ULS/WULS and CLS estimators. Noise variance=0.1 and DNR=41dB.

The constrained algorithm compared to the unconstrained algorithm, has a lower MSE for 4 to 8 anchors. For 8 to 12 anchors the performance shows a slightly lower MSE, and for more than 12 anchors, these two algorithms have the same performance. This difference is not significant, especially considering the greater computational complexity of the constrained algorithm. Therefore for simplicity is preferred to apply the weighting matrix to the unconstrained form. As expected, the weighted unconstrained estimator results in a lower MSE compared to the constrained, and the unweighted,

unconstrained estimators. It turns out that the latter two have very similar performance for large number of anchors.

Figure 2-9 shows MSE of the unconstrained, weighted unconstrained and constrained least square estimators versus DNR (dB) in 2D using TOA measurements for 10 and 20 anchors.

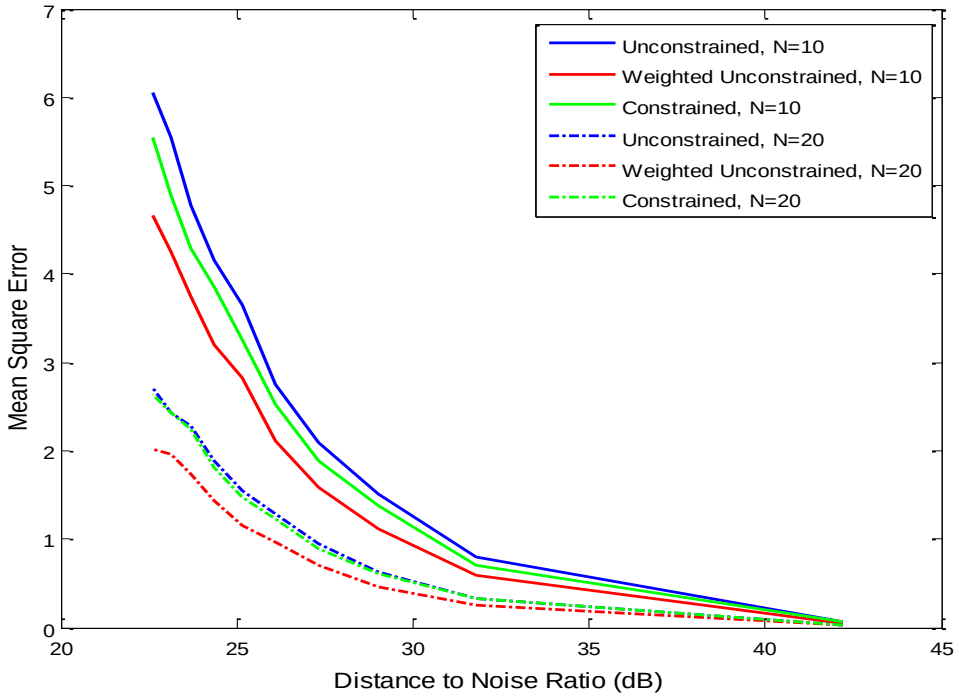

Figure 2-9. MSE vs. DNR (dB) in 2D using ULS/WULS and CLS estimator. The "Distance" is from the squared mean distance between the unlocalized node and the anchors averaged over an ensemble of 10^4 uniformly anchors distributions in a 100 by 100 square.

The LS estimator using more anchors results in a lower MSE. As seen above, the constrained and the unconstrained estimator have similar performance and the weight matrix improves the result of the estimator. The 10^4 realizations are on a 100 by 100 square and the noise variance varies 0.1 to 10.

2.5. Conclusions

In this chapter Least Squares was used as the estimator for the positioning. Computer simulations using MATLAB were conducted to evaluate the performance of the localization algorithm using TOA-based information. First, based on intuition, a new Nonlinear Least Squares Estimator (NLSE) was developed to estimate the position of an unknown node among some anchors. The Cramer-Rao lower bound (CRLB) was derived for the 1D case and the simulation result showed that for small levels of uncorrelated noise, the algorithm could attain almost zero bias, and the empirical curve became closer to the CRLB. Then, the algorithm was extended for the 2D case too. The NLSE takes longer than the LS estimator because of the need to solve two equations simultaneously, but it could get lower MSE.

The main idea of LS is to linearize the equations obtained from the TOA measurements. Then, constrained least squares (CLS) and weighted unconstrained least squares (WULS) were considered in order to solve the linear equations in an optimum manner. Lagrange multipliers were also used during this problem solving. It was suggested in the literature to apply the weight matrix to the constrained LS which would provide better performance than the unconstrained approach. However, the improvement of the constrained over the unconstrained algorithm was not that substantial, especially in view of its increased complexity. For simplicity the weighting matrix was applied to the unconstrained algorithm.

Comparison of these algorithms showed that weighted unconstrained LS could have lower MSE than the constrained, and the unconstrained LS. Also, the proposed nonlinear estimators could get similar results as the unconstrained estimator which was adapted from the literature.

Chapter 3: Localization Algorithms Using the Angular Data (AOA and DAOA Measurements)

Angle-of-arrival is another common location metric which is described and used for location estimation in many papers. In recent years, mainly due to the improvements and more presence of the antenna arrays using in the BSs of wireless communication networks, AOA measurements have attracted more attention in positioning problems [16][11]. Unfortunately, antenna arrays are not electrically compact devices. Optical frequencies (lasers) allow physically compact wireless AOA arrays.

In this chapter geometric techniques are reviewed for the localization of an unlocalized node using AOA information. Besides, a new angular measurement named DAOA is introduced in this chapter and a geometric algorithm is proposed for that. LOS propagation is assumed from the reference stations in order to establish geometric equations for position determination. All the clock of the anchors and the unlocalized node are synchronized.

This chapter is organized as follows. Section 3.1 introduces more detail about angle-based localization. Section 3.2 presents a closed form algorithm for AOA localization using two anchor nodes. In section 3.3, the unconstrained and weighted unconstrained least squares location algorithms using absolute AOA measurements are reviewed. In section 3.4, a new algorithm using differential AOA measurement is proposed to locate the unlocalized node. In order to evaluate the localization algorithm performances, simulation results are provided with each algorithm. Conclusions are drawn in section 3.5.

3.1. Introduction of Angle-Based Localization

Generally, AOA is the angle between the propagation direction of a signal and a reference direction, which is known as orientation [10][36]. The angle measurement indicates either the angle between two anchors from a reference node or the angle to a reference direction, or axis [20]. Both categories are considered in this chapter.

Angular measurements can support a TOA localization process or allow the nodes to be localized solely based on the angle information [20]. One common approach to obtain AOA measurement is to equip each sensor node with an antenna array or multiple receivers [10]. These requirements increase the cost of measurement.

Figure 3-1, represents three BSs and their axes. It shows that the AOA of the transmitted signal, for example, by C (or A) to B is α (or β). ψ is the heading angle or the *orientation* of the system that is formed by the sensor axis and North, in a clockwise direction. ψ defines a fixed direction against which the AOAs are measured [10][17]. In other words, this orientation or ψ is the angular displacement of the sensor-based coordinate system and the geographic coordinates. The AOA is called absolute AOA whenever the orientation is zero or pointing to North, otherwise, it is called relative [10].

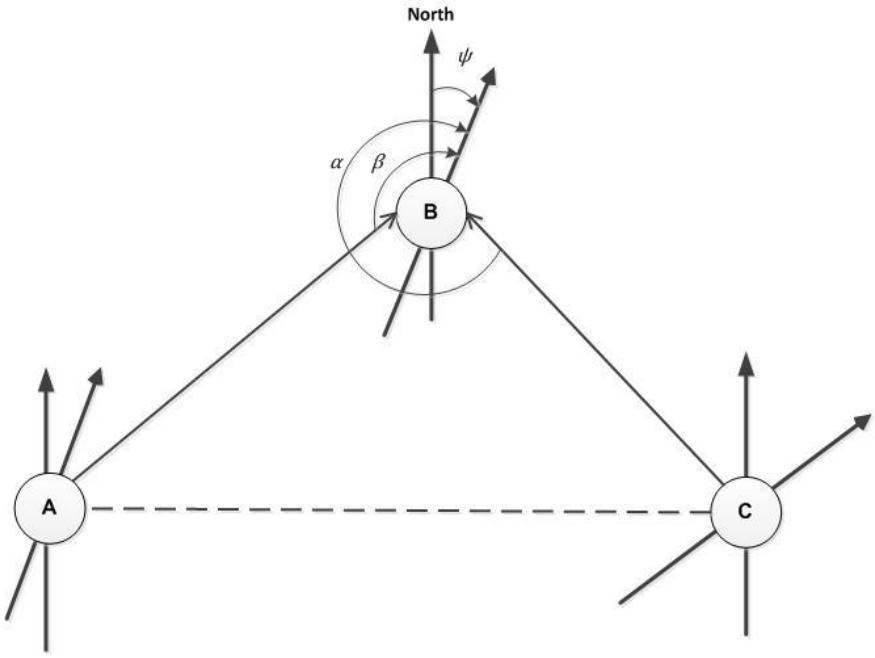

Figure 3-1. Definition of AOA (adapted from [17]). (Node B with its heading and incoming angles from A and C).

The position of the unlocalized node can be estimated by using at least two lines of bearing (LOB) which are drawn from the anchor node to the unlocalized node. This estimate is undertaken for each AOA measurement [7][20].

There is also an option to combine the angle information from AOA with knowledge of distances from TOA measurements. This is called a hybrid technique which should increase the accuracy of the localization and is reviewed in the next chapter of this thesis. This improved accuracy makes AOA technique an attractive positioning method despite its cost and difficulty of deploying large (i.e., directional) antennas [20].

Requirement of large and complex antenna arrays and direction of arrival estimation at the BSs are some of the disadvantages of AOA algorithms. In order to have an accurate positioning, the angle measurement needs to have consummate accuracy. Therefore, using optical technology can be an option for angular measurements.

3.2. Closed Form for AOA Localization Using Two Anchors

For AOA measurements, two anchors are sufficient to determine the position of the unlocalized node by intersecting two lines, which is called *triangulation* (Figure 3-2) [4][36].

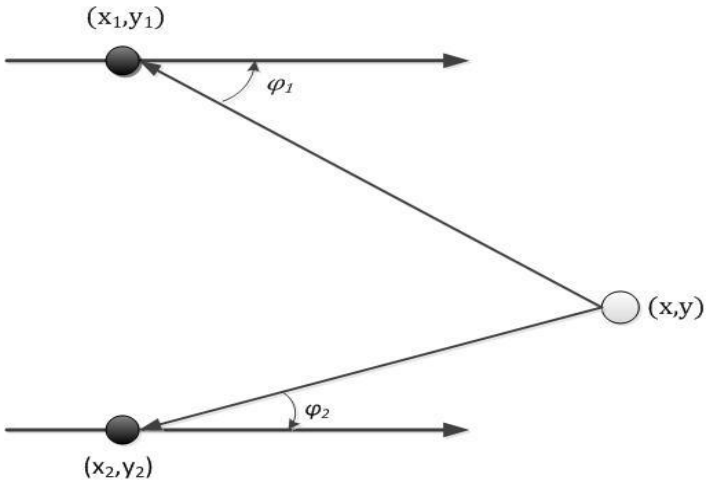

Figure 3-2. Definition of triangulation (adapted from [4]). The angles measured by the reference nodes (black nodes) determine two lines, the intersection of which yields the target position.

Let φ_1 and φ_2 denote the angles measured by anchors 1 and 2 to the same axis, respectively. Then, the following two equations are solved for the position of the target [4]:

$$tan\,\varphi_1 = \frac{y - y_1}{x - x_1} \quad and \quad tan\,\varphi_2 = \frac{y - y_2}{x - x_2} \tag{3-1}$$

which yields the x and y position of the unknown point:

$$x = \frac{x_2\,tan\,\varphi_2 - x_1\,tan\,\varphi_1 + y_1 - y_2}{tan\,\varphi_2 - tan\,\varphi_1} \tag{3-2}$$

$$y = \frac{(x_2 - x_1)\tan\varphi_1\tan\varphi_2 + y_1\tan\varphi_2 - y_2\tan\varphi_1}{\tan\varphi_2 - \tan\varphi_1} \quad (3\text{-}3)$$

So, just having the position information of two anchor nodes leads to a closed form of localization of the third node.

3.3. Using Absolute Bearing Measurement of AOA for More than Two Anchor Nodes

In this section, the sensor coordinates are aligned with geographic coordinates. So, the absolute bearing refers to geographic coordinates. In the previous section, the AOA localization algorithm was considered using just two anchors. However, in general, in order to present a formula for the AOA of the transmitted signal from the MS at the i-*th* BS, equation (3-1) can be used, and for M BSs is:

$$\tan(\varphi_i) = \frac{y - y_i}{x - x_i}, \quad i = 1,2,\dots,M. \quad (3\text{-}4)$$

Equation (3.4) shows that φ_i is the angle between the line of bearing (LOB) from the i-th anchor to the unlocalized node and the x-axis, and it is recalled that with the sensor coordinates aligned with geographic coordinates, then the sensor axis is also along the x-axis [7]. The measurement of AOA is denoted by $\{\alpha_{AOA,i}\}$ which is modeled with additive noise [7]:

$$\alpha_{AOA,i} = \varphi_i + n_{AOA,i} = \tan^{-1}\left(\frac{y - y_i}{x - x_i}\right) + n_{AOA,i}, \quad i = 1,2,\dots,M. \quad (3\text{-}5)$$

where $n_{AOA,i}$ is the noise in $\alpha_{AOA,i}$.

Equation (3-5) can also be expressed in vector form as:

$$\boldsymbol{\alpha}_{AOA} = \boldsymbol{f}_{AOA}(x) + \boldsymbol{n}_{AOA}, \tag{3-6}$$

where

$$\boldsymbol{\alpha}_{AOA} = [\alpha_{AOA,1}\ \alpha_{AOA,2} \dots\ \alpha_{AOA,M}]^T, \tag{3-7}$$

$$\boldsymbol{f}_{AOA}(\boldsymbol{x}) = \begin{bmatrix} tan^{-1}(\frac{y-y_1}{x-x_1}) \\ tan^{-1}(\frac{y-y_2}{x-x_2}) \\ \vdots \\ tan^{-1}(\frac{y-y_M}{x-x_M}) \end{bmatrix}, \tag{3-8}$$

where $\boldsymbol{x} = [x \quad y]^T$.

For the development and analysis of the proposed (in [7]) location algorithm using AOA, an assumption is now made about the measurement error, viz., that it is sufficiently small (i.e., high SNR case) and modeled as zero mean Gaussian. The noise covariance matrix is denoted $\boldsymbol{C}_{\boldsymbol{n},AOA}$ [7]**.**

3.3.1. Algorithm development [7]

In order to make the calculations simpler, the $\alpha_{AOA,i}$ measurements are considered, for now, without noise [7], i.e.

$$tan(\alpha_{AOA,i}) = \frac{sin(\alpha_{AOA,i})}{cos(\alpha_{AOA,i})} = \frac{y-y_i}{x-x_i}, \quad i = 1,2,\dots,M. \tag{3-9}$$

Rearranging the above equation yields

$$x\sin(\alpha_{AOA,i}) - y\,cos(\alpha_{AOA,i}) = x_i\sin(\alpha_{AOA,i}) - y_i\,cos(\alpha_{AOA,i}),$$
$$i = 1,2,\dots,M. \tag{3-10}$$

The same matrix-vector form as for TOA in the previous chapter is used here for AOA:

$$\boldsymbol{Hx} = \boldsymbol{k}\,, \tag{3-11}$$

where

$$\boldsymbol{H} = \begin{bmatrix} sin(\alpha_{AOA,1}) & -cos(\alpha_{AOA,1}) \\ \vdots & \vdots \\ \sin(\alpha_{AOA,M}) & -cos(\alpha_{AOA,M}) \end{bmatrix}, \tag{3-12}$$

$$\boldsymbol{k} = \begin{bmatrix} x_1\,sin(\alpha_{AOA,1}) - y_1\,cos(\alpha_{AOA,1}) \\ \vdots \\ x_M\,sin(\alpha_{AOA,M}) - y_M\,cos(\alpha_{AOA,M}) \end{bmatrix}. \tag{3-13}$$

Location of the unlocalized node ($\boldsymbol{x} = [x \quad y]^T$) can be estimated using LSE. At this point, all the measurement elements are equally weighted. However, the LS estimator will perform better if different weights are used. The performance, with and without a weighting matrix (i.e., WLS), is shown here [7]. The LS estimator is

$$\hat{\boldsymbol{x}} = argmin_{\boldsymbol{x}}(\boldsymbol{Hx} - \boldsymbol{k})^{\boldsymbol{T}}(\boldsymbol{Hx} - \boldsymbol{k}) = (\boldsymbol{H^T H})^{-1}\boldsymbol{H^T k} \tag{3-14}$$

Equation (3-14) is similar to equation (2-31) which was the solution in [7] for the unconstrained approach for using TOA measurements in the previous chapter.

Finding an optimum weighting matrix, $\boldsymbol{\Omega^{-1}}$, is determined in [7] based on the BLUE technique. The estimated position of the unlocalized node is

$$\begin{aligned}\hat{\boldsymbol{x}} &= argmin_{\boldsymbol{x}}(\boldsymbol{H}\boldsymbol{x}-\boldsymbol{k})^{\boldsymbol{T}}\boldsymbol{\Omega}^{-\mathbf{1}}(\boldsymbol{H}\boldsymbol{x}-\boldsymbol{k}) \\ &= (\boldsymbol{H}^T\boldsymbol{\Omega}^{-1}\boldsymbol{H})^{-1}\,\boldsymbol{H}^T\,\boldsymbol{\Omega}^{-1}\,\boldsymbol{k}\,.\end{aligned} \tag{3-15}$$

Following [7], by considering small errors, and expanding sin and cos functions in (3-10) such that $sin(n_{AOA,i}) \approx n_{AOA,i}$ and $cos(n_{AOA,i}) \approx 1$, the equation reduces to

$$\begin{aligned}&x\,sin(\phi_i + n_{AOA,i}) - y\,cos(\phi_i + n_{AOA,i}) \\ &= x_i\,sin(\phi_i n_{AOA,i}) - y_i\,cos(\phi_i + n_{AOA,i}), \\ &\qquad i = 1,2,\dots,M.\end{aligned} \tag{3-16}$$

In order to determine the optimum $\boldsymbol{\Omega}$, the residual error in $\alpha_{AOA,i}$ is required [7], i.e.

$$\delta_i = n_{AOA,i}\,[(x-x_i)\,cos(\phi_i) + (y-y_i)sin(\phi_i)],\;\; i = 1,2,\dots,M. \tag{3-17}$$

In vector form, $\{\delta_i\}$ is

$$\boldsymbol{\delta} = \begin{bmatrix} n_{AOA,1}\,[(x-x_1)\,cos(\phi_1) + (y-y_1)sin(\phi_1)] \\ n_{AOA,2}\,[(x-x_2)\,cos(\phi_2) + (y-y_2)sin(\phi_2)] \\ \vdots \\ n_{AOA,M}\,[(x-x_M)\,cos(\phi_M) + (y-y_M)sin(\phi_M)] \end{bmatrix}. \tag{3-18}$$

Thus the inverse of the optimum weighting matrix is:

$$\boldsymbol{\Omega}^0 = E\{\boldsymbol{\delta}\boldsymbol{\delta}^T\} = \boldsymbol{m}\boldsymbol{m}^T \odot C_{\boldsymbol{n},AOA}\,. \tag{3-19}$$

where

$$\boldsymbol{m} = \begin{bmatrix} (x - x_1)\,cos(\phi_1) + (y - y_1)sin(\phi_1) \\ (x - x_2)\,cos(\phi_2) + (y - y_2)sin(\phi_2) \\ \vdots \\ (x - x_M)\,cos(\phi_M) + (y - y_M)sin(\phi_M) \end{bmatrix} = \begin{bmatrix} d_1 \\ d_2 \\ \vdots \\ d_M \end{bmatrix}. \quad (3\text{-}20)$$

$\boldsymbol{m}$ is determined as (3-20) because $cos(\phi_i) = \frac{(x - x_i)}{d_i}$ and $sin(\phi_i) = \frac{(y - y_i)}{d_i}$ [7].

In summary, the various measurements of angle are weighted inversely to their noise power. This means that those measurements with high SNR are emphasised, and those with low SNR are de-emphasized. The combination technique is also called maximum ratio combining, which gives the best resultant SNR of all linear combinations. The output SNR is the sum of the measurement SNRs.

Simulation Results

In this section simulation results are provided. Figure 3-3 shows the behaviors in the form of MSE of the LS estimator and the weighted LS, versus number of anchors. Since matrix H in AOA has dimension $M \times 2$, in order to have full rank matrix, M should be greater than or equal to 2. (The MSE for using 3 anchors is 5.6 and 5.2 for LS and WLS respectively.) Noise is Gaussian with variance of 2 degrees^2 and the anchors are uniformly distributed over a 100 by 100 square area.

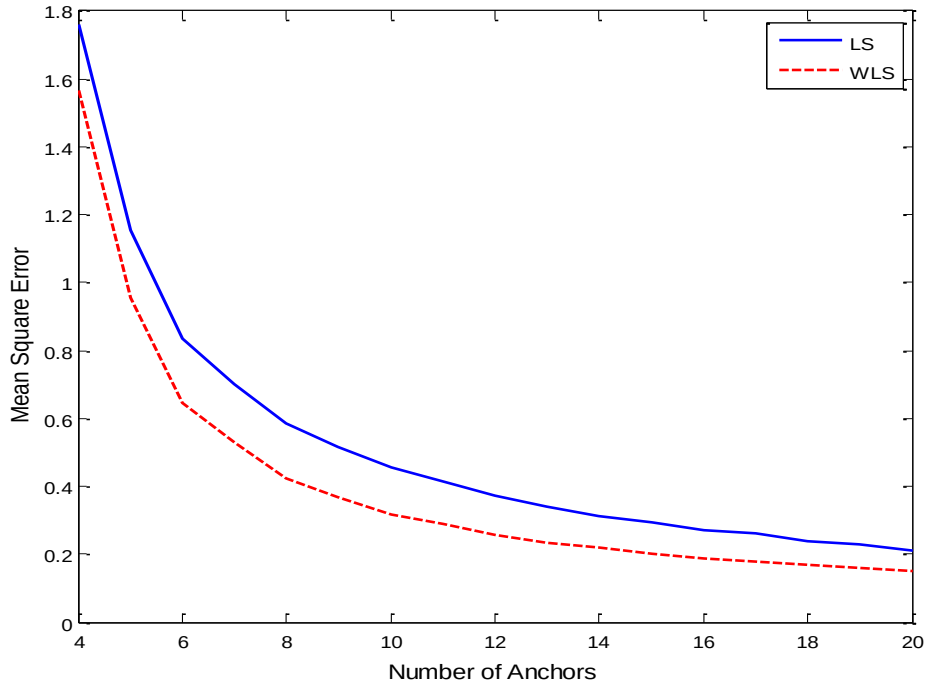

Figure 3-3. MSE vs. number of anchors for LS/WLS using AOA measurements. A square of 100 by 100 contains the uniformly distributed anchors. Angle noise is Gaussian with variance of 2 degrees^2.

Figure 3-3 shows how increasing the number of anchors, up to 12, lowers the MSE, for this geometry. Diminishing returns cut in when more than about 12 anchors are used and, as expected, WLS has better performance than the LS estimator for the same noise variance. This is akin to maximum ratio combining of the observations and equal gain combining of the observations.

Figure 3-4 shows the MSE of the LS estimator and the WLS, using 20 anchors, versus angle noise variance.

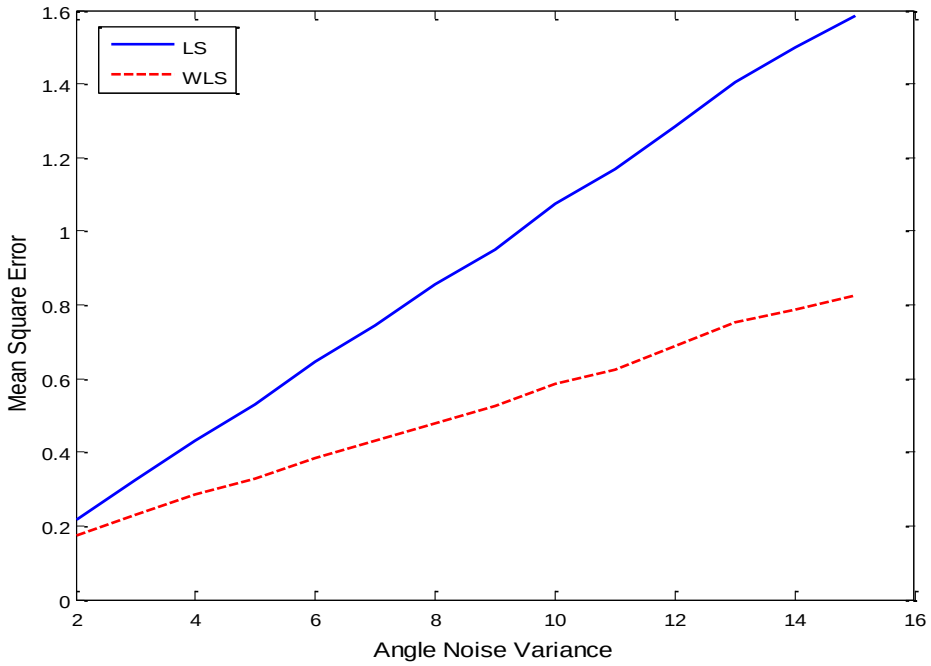

Figure 3-4. MSE vs. angle noise variance (in degrees^2) for LS/WLS using AOA measurements.

It illustrates how increasing the angle noise variance causes a larger estimation error.

3.4. Differential Angle of Arrival measurement (DAOA)

In some systems, a new scenario of using angular information can be described for localization of the unknown node. In the previous sections of this chapter, algorithms for using AOA measurements were reviewed. In this section, a new algorithm is proposed using DAOA. The unlocalized node is supposed to be at the centre of a circular locus of anchors. The estimation of the unlocalized node's location is studied here by using the angle subtending two anchors from the unlocalized node. These angles can be considered as the differential AOA between two anchors which is why it is called DAOA. DAOA has the advantage of not needing to know the absolute angles (i.e., orientation, cf., Figure 3-1) of the sensors. The DAOA measurement is motivated by using rotating laser technology.

By using the triangulation technique (cosine law), the distances between nodes (nodes A and B in Figure 3-5) which are not in the same transmission direction, can be computed. From Figure 3-5, the cosine law is:

$$c^2 = a^2 + b^2 - 2\,a\,b\,cos(\gamma)\,. \tag{3-21}$$

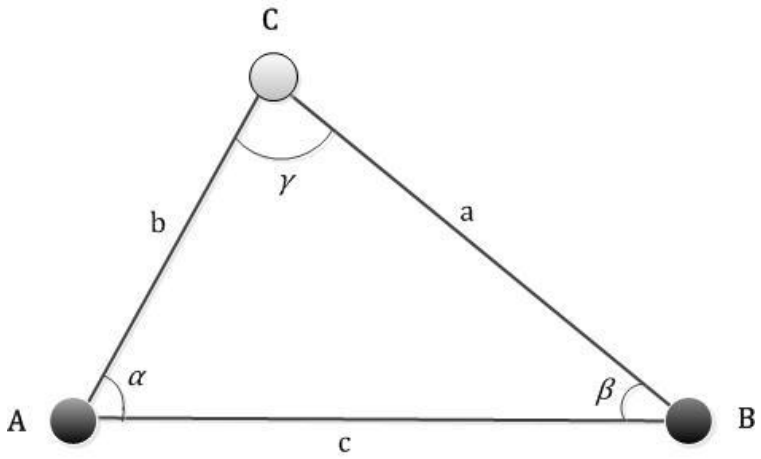

Figure 3-5. Representation of DAOA. A and B are the anchors, and C is the unlocalized node. γ is the DAOA. In order to solve in closed form, "a" should equal "b".

For a closed form solution, a circular configuration must be assumed for the anchors, i.e., the anchors are all on a circle with the unlocalized node at the centre. For node C (with (x, y) coordinates) being the unknown node in Figure 3-5, and *a=b,* then

$$c^2 = 2a^2 - 2a^2\cos(\gamma)\,, \tag{3-22}$$

which leads to

$$a^2 = \frac{c^2}{2(1-\cos(\gamma))}. \tag{3-23}$$

If (x_i, x_i) is considered as the coordinates of node B, for more nodes, the coordinates of node A would be denoted by (x_{i+1}, y_{i+1}) and the M-th point has the coordinates of (x_M, y_M). So, (3-23) becomes

$$(x - x_i)^2 + (y - y_i)^2 = \frac{c_{i,i+1}^2}{2\big(1 - cos(\gamma_{i,i+1})\big)}, \tag{3-24}$$

where $\gamma_{i,i+1}$ and $c_{i,i+1}$ denoted the angle and distance between i-th and $(i+1)$-th anchor node respectively. Expanding the left side of equation (3-24) gives:

$$x^2 + y^2 - 2xx_i - 2yy_i + \big(x_i^2 + y_i^2\big) = \frac{c_{i,i+1}^2}{2\big(1 - \cos(\gamma_{i,i+1})\big)}. \tag{3-25}$$

Rearranging (3-25) gives:

$$\begin{aligned} xx_i + yy_i - 0.5R^2 &= \frac{1}{2}\big(x_i^2 + y_i^2\big) - \frac{1}{4}\left(\frac{c_{i,i+1}^2}{1 - cos(\gamma_{i,i+1})}\right), \\ xx_i + yy_i - 0.5R^2 &= \frac{1}{2}\left(x_i^2 + y_i^2 - \frac{c_{i,i+1}^2}{2(1 - cos(\gamma_{i,i+1}))}\right), \\ R^2 &= x^2 + y^2. \end{aligned} \tag{3-26}$$

Now, (3-26) has a familiar form, viz., like equation (2-28) for TOA measurement. So, matrix-vector form of $\boldsymbol{A\theta} = \boldsymbol{b}$ in (2-29) is useful here again. Vector $\boldsymbol{\theta} = \begin{bmatrix} x \\ y \\ R^2 \end{bmatrix}$ is the same as before, but matrix $\boldsymbol{A}$ and the vector $\boldsymbol{b}$ change to:

$$\boldsymbol{A} = \begin{bmatrix} x_1 & y_1 & -0.5 \\ \vdots & \vdots & \vdots \\ x_{M-1} & y_{M-1} & -0.5 \end{bmatrix}, \boldsymbol{b} = \frac{1}{2}\begin{bmatrix} x_1^2 + y_1^2 - \dfrac{c_{1,2}^2}{2(1-cos(\gamma_{1,2}))} \\ \vdots \\ x_{M-1}^2 + y_{M-1}^2 - \dfrac{c_{M-1,M}^2}{2(1-cos(\gamma_{M-1,M}))} \end{bmatrix}. \quad (3\text{-}27)$$

Similar to TOA, the DAOA can be solved by unconstrained LS similar to (2-31) with $\boldsymbol{A}$ and $\boldsymbol{b}$ in (3-27). Since it was shown in the previous chapter that constrained LS had almost the same simulation result with higher complexity, it is not considered as an option in this section and unconstrained LS is used as the estimator here.

Figure 3-6 shows the MSE against the number of anchors for the simulation result of the unconstrained LS using DAOA measurements. The angle noise is Gaussian with variance of 4 degrees^2. Since matrix A in DAOA has $(M-1)\times 3$ dimension, in order to have full rank matrix, $(M-1)$ should be greater than or equal to 3. Thus, M should be greater than or equal to 4.

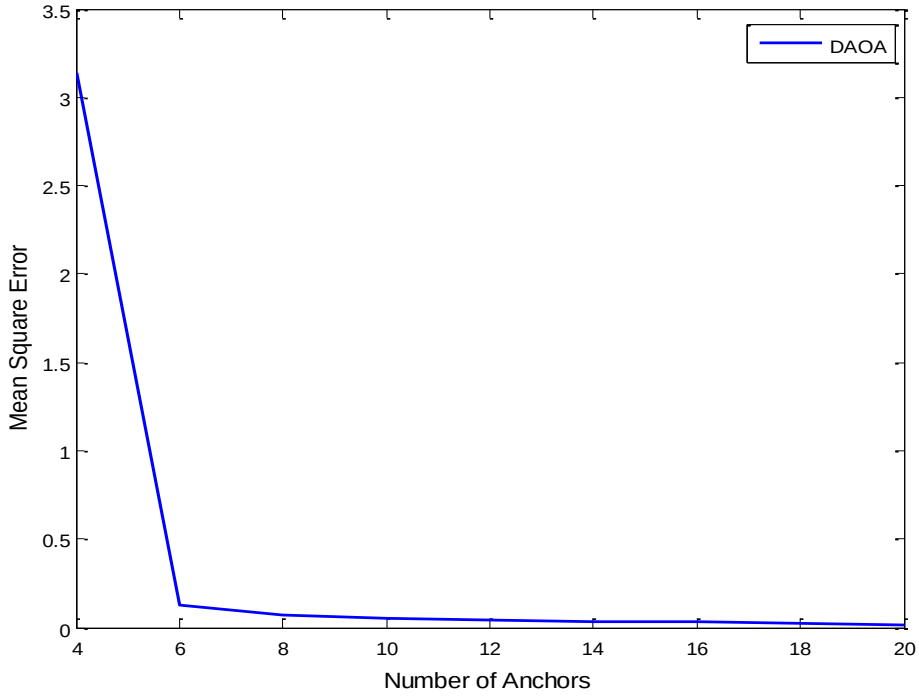

Figure 3-6. MSE vs. number of anchors for unconstrained least square estimator using DAOA measurements. Anchors are on a circle with radius 10 around the unknown node, and angular noise variance of 4 degrees^2.

This figure shows that adding more than 8 anchors to the system would change the performance only slightly. For example, when 10 anchors are used, the MSE is about 0.05, and for 20 anchors, the MSE is about 0.02. It is emphasized that these results stem from a specific arrangement for the anchors.

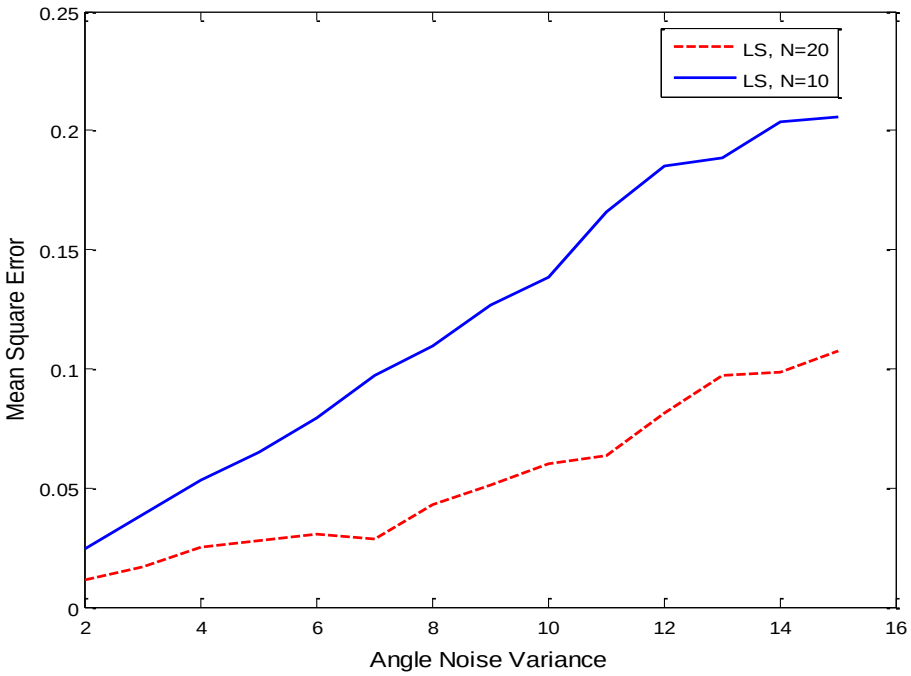

Figure 3-7. MSE vs. angle noise variance for unconstrained least squares estimator using DAOA. Anchors are on a circle with radius 10 around the unknown node.

In Figure 3-7, angle noise variances of 2 to 16 degrees^2 are used to show the impact on the accuracy. Tie points are: for a noise variance of 8, the MSE is about 0.1 and 0.03 for LS estimator using 10 and 20 anchors respectively.

3.5. Conclusions

In this chapter, localization of an unknown node in a wireless sensor network using angle-based observations was presented. The unknown sensor was assumed to be capable of detecting angles of the incidence signal from the anchors. Least Squares used as the estimator and computer simulations using MATLAB were used to evaluate the algorithms.

The algorithm which was reviewed for AOA measurement used unconstrained and weighted unconstrained LS estimator. WLS could achieve a better result compared to LS.

A new DAOA-based positioning method has been introduced in this chapter. The remarkable feature of this method was its capability of accurate localization from purely DAOA information, which is a new concept. The significance is that DAOA can be easier to obtain than AOA in some situations. The algorithm was evaluated using a specific deployment (circular) of the anchors; however this is not a fundamental limitation. But this specific situation also provided a closed-form solution to the location problem. Simulation results showed that applying more than 8 anchor nodes on a circle sees diminishing returns for the location accuracy.

Chapter 4: Localization Algorithms Using Hybrid Technique

The combination of different positioning techniques should be able to improve accuracy and loosen constraints on the physical layout of the localization problem. In the literature this type of combination of techniques is also called data fusion or hybrid technique [18]. Another motivation of employing a hybrid technique is to reduce the number of required anchors for a given localization performance [22].

In this chapter, the TDOA/AOA hybrid technique is reviewed and a new TOA/DAOA technique is introduced. Since TDOA measurement and its formulations have not described in the previous chapters of this thesis, in section 4.1 it is briefly reviewed. In section 4.2 and 4.3, hybrid localization techniques comprising TDOA/AOA and TOA/DAOA are discussed respectively. Hybrid localization in three-dimensions is an interesting problem which is reviewed in section 4.4. Finally, conclusions are drawn in section 4.5.

4.1. Review of TDOA Algorithm

The idea of TDOA is to determine the relative position of the unknown node by examining only the difference in time at which the transmitted signal arrives at different anchors, rather than the absolute arrival time of TOA [3]. (Clearly if the pairs of absolute TOAs are known, then their TDOAs can be calculated.) The unknown sensor does not need to be synchronized with the anchors, but the anchors must be tightly synchronized [13]. There are methods, e.g. [3][23], for measuring the TDOA. Each TDOA measurement defines a hyperbolic locus on which the unlocalized node must lie. A 2D target location estimate is given by the intersection of two or more locii as shown in Figure 4-1 [3].

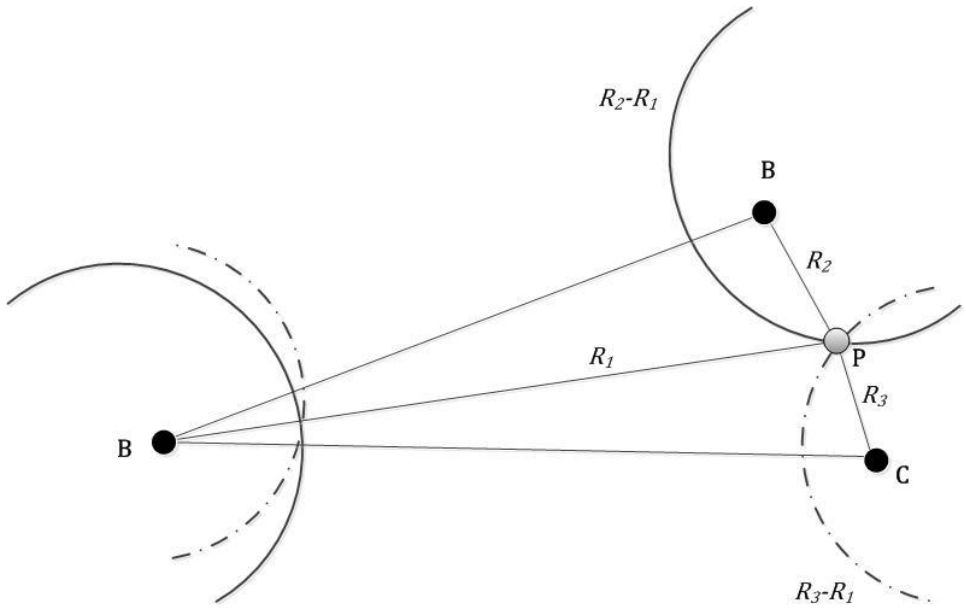

Figure 4-1. Positioning based on TDOA Measurements (adapted from [3]). A, B, and C are anchors and P is the unknown node.

The intersection of two hyperbolas formed from TDOA measurements of three anchors (A, B, and C), gives the location of the unknown node (for example, node P in Figure 4-1).

4.1.1. TDOA Formulation

TDOA is the difference in TOAs of the transmitted signal from the unknown sensor at a pair of anchors. So, if the first anchor is assigned as a reference point, the range measurements based on the TDOAs are of the form [3][7]

$$r_{TDOA,i} = (d_i - d_1) + n_{TDOA,i}$$

$$= \sqrt{(x - x_i)^2 + (y - y_i)^2} - \sqrt{(x - x_1)^2 + (y - y_1)^2} + n_{TDOA,i}, \quad i = 2,3,\dots,M. \tag{4-1}$$

where the range error, $n_{TDOA,i}$, can be obtained from the difference of two TOA noise. So, $n_{TDOA,i}$ is $n_{TOA,i} - n_{TOA,i-1}$, $i = 2,3,\dots,M$. In vector form, the range measurements in (4-1) become [7]:

$$\boldsymbol{r}_{TDOA} = \boldsymbol{f}_{TDOA}(\boldsymbol{x}) + \boldsymbol{n}_{TDOA}, \tag{4-2}$$

where

$$\boldsymbol{r}_{TDOA} = [r_{TDOA,2}\ r_{TDOA,3} \dots r_{TDOA,M}]^T, \tag{4-3}$$

$$\boldsymbol{n}_{TDOA} = [n_{TDOA,2}\ n_{TDOA,3} \dots n_{TDOA,M}]^T, \tag{4-4}$$

$$\boldsymbol{f}_{TDOA}(\boldsymbol{x}) = \begin{bmatrix} \sqrt{(x-x_2)^2 + (y-y_2)^2} - \sqrt{(x-x_1)^2 + (y-y_1)^2} \\ \sqrt{(x-x_3)^2 + (y-y_3)^2} - \sqrt{(x-x_1)^2 + (y-y_1)^2} \\ \vdots \\ \sqrt{(x-x_M)^2 + (y-y_M)^2} - \sqrt{(x-x_1)^2 + (y-y_1)^2} \end{bmatrix}, \tag{4-5}$$

where $\boldsymbol{x} = [x \quad y]^T$.

4.1.2. Algorithm Development

For high SNR, the corresponding nonlinear equations which are obtained from TDOA measurements can be linearized. The technique is commonly called spherical interpolation (SI) that solves the linear equations using LS estimator [30]. The procedure is the same as what was described for TOA measurements in chapter 2.

In order to develop the CLS/ULS mobile positioning estimator using the TDOA data as it is discussed in [7], equation (4-1) can be considered without noise.

$$r_{TDOA,i} = \sqrt{(x-x_i)^2 + (y-y_i)^2} - \sqrt{(x-x_1)^2 + (y-y_1)^2}. \tag{4-6}$$

Rearranging the above equation leads to

$$r_{TDOA,i} + \sqrt{(x - x_1)^2 + (y - y_1)^2} = \sqrt{(x - x_i)^2 + (y - y_i)^2},$$
$$i = 2,3, \dots, M. \tag{4-7}$$

An intermediate variable, R_1, is introduced here which has the form

$$R_1 = d_1 = \sqrt{(x - x_1)^2 + (y - y_1)^2}. \tag{4-8}$$

Squaring both sides of (4-7) and using R_1 , then rearranging the equation gives the following set of linear equations [7]

$$(x - x_1)(x_i - x_1) + (y - y_1)(y_i - y_1) + r_{TDOA,i} R_1$$
$$= \frac{1}{2}\left[(x_i - x_1)^2 + (y_i - y_1)^2 - r_{TDOA,i}^2\right], \qquad i = 2,3, \dots, M. \tag{4-9}$$

(4-9) in matrix form is

$$\boldsymbol{G\vartheta} = \boldsymbol{h}, \tag{4-10}$$

where

$$\boldsymbol{G} = \begin{bmatrix} x_2 - x_1 & y_2 - y_1 & r_{TDOA,2} \\ \vdots & \vdots & \vdots \\ x_M - x_1 & y_M - y_1 & r_{TDOA,M} \end{bmatrix},$$
$$\boldsymbol{h} = \frac{1}{2}\begin{bmatrix} (x_2 - x_1)^2 + (y_2 - y_1)^2 - r_{TDOA,2}^2 \\ \vdots \\ (x_M - x_1)^2 + (y_M - y_1)^2 - r_{TDOA,M}^2 \end{bmatrix}, \tag{4-11}$$

also $\boldsymbol{\vartheta}$ is the parameter vector which consists of the unlocalized node location as well as R_1 ($\boldsymbol{\vartheta} = [x - x_1, y - y_1, R_1]^T$).

LS is used to solve (4-10) in the presence of noise, and to estimate the location of the unlocalized node [30]:

$$\widehat{\boldsymbol{\vartheta}} = argmin_{\boldsymbol{\vartheta}} \, (\boldsymbol{G\vartheta} - \boldsymbol{h})^T (\boldsymbol{G\vartheta} - \boldsymbol{h}) = (\boldsymbol{G}^T \boldsymbol{G})^{-1} \boldsymbol{G}^T \boldsymbol{h}, \tag{4-12}$$

where

$$\boldsymbol{\vartheta} = \begin{bmatrix} x - x_1 \\ y - y_1 \\ R_1 \end{bmatrix} \tag{4-13}$$

without utilizing the known relationship between x, y, and R_1 [7].

In order to improve the SI estimator, the LS cost function in (4-12) can be solved subject to the constraint [7]:

$$\boldsymbol{\vartheta}^T \boldsymbol{\Sigma} \boldsymbol{\vartheta} = 0, \tag{4-14}$$

where $\boldsymbol{\Sigma}$ is $diag(1, 1, -1)$.

As mentioned earlier in the previous chapters, using WLS helps to improve the estimation. So, using $\boldsymbol{\Upsilon}^{-1}$ as a symmetric weighting matrix changes the LS to [7]

$$\widehat{\boldsymbol{\vartheta}} = argmin_{\boldsymbol{\vartheta}} (\boldsymbol{G\vartheta} - \boldsymbol{h})^T \boldsymbol{\Upsilon}^{-1} (\boldsymbol{G\vartheta} - \boldsymbol{h}), \tag{4-15}$$

Finding the optimum weighting matrix procedure is similar to TOA and AOA mentioned in the previous chapters and it is not mentioned here again.

4.2. Hybrid TDOA/AOA

It has been mentioned in the literature, e.g. [23], that combining different techniques can improve location performance and/or reduce the number of receiving

anchors in the system. Among various hybrid schemes, the most popular one is to use the TDOA and AOA measurements simultaneously [17][22][23].

To perform TDOA/AOA mobile positioning, (3-10) is now rewritten by adding $y_1\, cos(\alpha_{AOA,i}) - x_1\, sin(\alpha_{AOA,i})$ on both sides [7]:

$$\begin{aligned}&(x - x_1)\, sin(\alpha_{AOA,i}) - (y - y_1)\, cos(\alpha_{AOA,i}) \\ &\quad = (x_i - x_1)\, sin(\alpha_{AOA,i}) - (y_i - y_1)\, cos(\alpha_{AOA,i}), \quad i = 1,2, \dots, M.\end{aligned} \tag{4-16}$$

Combining (4-9) and (4-16) into a single matrix-vector form yields [7]

$$\boldsymbol{B\vartheta} = \boldsymbol{w}, \tag{4-17}$$

where [7]

$$\boldsymbol{B} = \begin{bmatrix} \boldsymbol{G} \\ \boldsymbol{H} \quad \boldsymbol{0_M} \end{bmatrix}, \qquad \boldsymbol{w} = \begin{bmatrix} \boldsymbol{h} \\ \boldsymbol{l} \end{bmatrix}, \tag{4-18}$$

$$\boldsymbol{l} = \begin{bmatrix} 0 \\ (x_2 - x_1)\, sin(\alpha_{AOA,2}) - (y_2 - y_1)\, cos(\alpha_{AOA,2}) \\ \vdots \\ (x_M - x_1)\, sin(\alpha_{AOA,M}) - (y_M - y_1)\, cos(\alpha_{AOA,M}) \end{bmatrix}, \tag{4-19}$$

where $\boldsymbol{0}_M$ is an $M \times 1$ column vector with all zeros and $\boldsymbol{G}$ and $\boldsymbol{h}$ are the same matrix and vector as defined in (4-11) and $\boldsymbol{H}$ defines in (3-12). Then $\boldsymbol{\vartheta}$ is solved by

$$\widehat{\boldsymbol{\vartheta}} = arg\, min_{\boldsymbol{\vartheta}} (\boldsymbol{B\vartheta} - \boldsymbol{w})^T \boldsymbol{W^{-1}} (\boldsymbol{B\vartheta} - \boldsymbol{w}) = (\boldsymbol{B^T W^{-1} B})^{-1}\, \boldsymbol{B^T}\, \boldsymbol{W^{-1}}\, \boldsymbol{w}, \tag{4-20}$$

where $\boldsymbol{W}^{-1}$ is the weighting matrix. The constrained LS estimate of $\boldsymbol{\vartheta}$ is obtained by minimizing the cost function in (4-20), subject to [7]

$$\boldsymbol{\vartheta}^T \boldsymbol{\Sigma} \boldsymbol{\vartheta} = 0. \quad (4\text{-}21)$$

Parameters $\boldsymbol{\Sigma}$ and $\boldsymbol{\vartheta}$ are the same as defined before. The details on this technique are similar to the TDOA or TOA techniques.

4.3. Hybrid TOA/DAOA

In this section, a new hybrid algorithm is developed for localization. The noisy distances between the anchors to the unknown node (TOA measurements) and the DAOA measurements, are used for this algorithm. Figure 4-2 depicts the situation.

The distances between the anchors to the unknown node are found from propagation time measurement. The angles between the anchors would be measured using a laser. In fact, the DAOA and hybrid TOA/DAOA are introduced in this thesis motivated by using rotating laser technology.

The cosine law (3-21) is again used. Similar to the previous chapters, all the anchors are assumed to be distributed uniformly over a 100 by 100 square. The measurement noises are zero-mean Gaussian with variance of 0.1 for distances, and angular variance of 2 degrees^2.

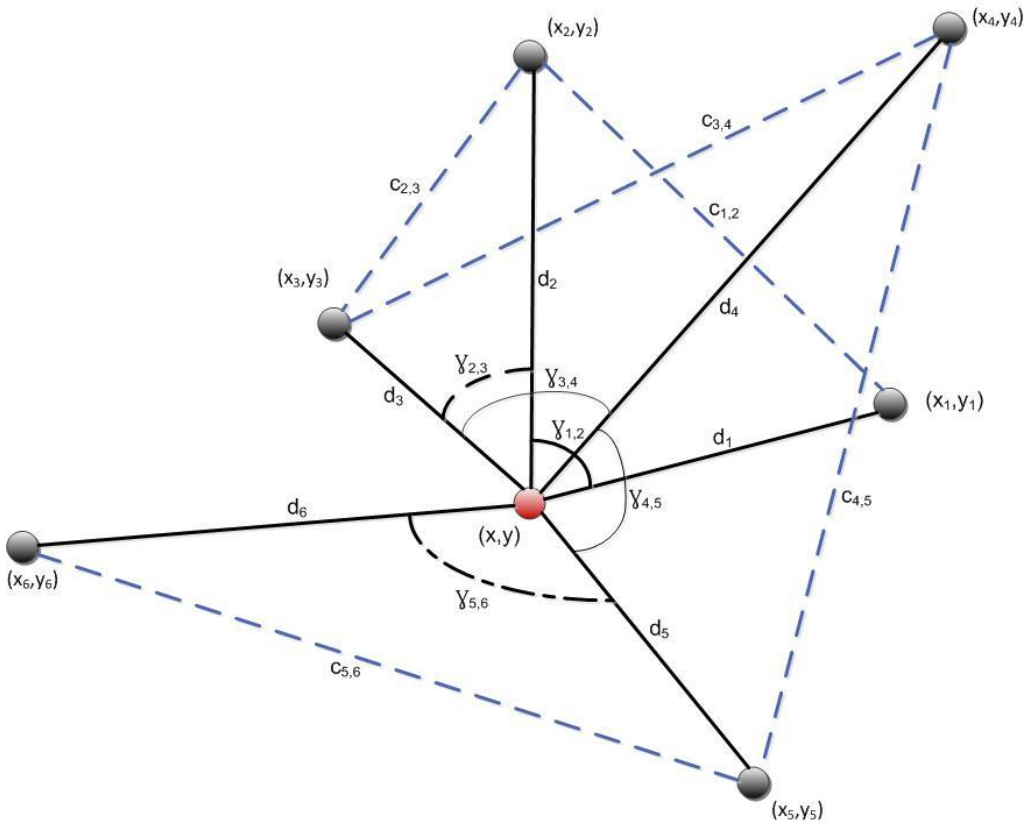

Figure 4-2. Representation of an unknown node and some randomly distributed anchors. $\gamma_{i,j}$ is DAOA and $c_{i,j}$ is the distance between i-th and j-th anchor. d_i is the distance of i-th anchor to the unknown node.

The distances between two consecutive random anchors ($c_{i,i+1}$) can be calculated as below

$$c_{i,i+1}^2 = (x - x_i)^2 + (y - y_i)^2 + (x - x_{i+1})^2 + (y - y_{i+1})^2 - 2d_i d_{i+1} \cos(\gamma_{i,i+1}), \quad i = 1,2,\dots,M, \tag{4-22}$$

where (x, y) and (x_i, y_i) are the unknown node and an anchor coordinates respectively. d_i is the noisy distance of the i-th anchor to the unknown node and $\gamma_{i,i+1}$ is the noisy DAOA between i-th and $i+1$-th anchor. Expanding (4-22) and rearranging it shows in (4-23),(4-24), and (4-25).

$$c_{i,i+1}^2 = x^2 + x_i^2 - 2xx_i + y^2 + y_i^2 - 2yy_i + x^2 + x_{i+1}^2 - 2xx_{i+1} + y^2 + y_{i+1}^2 - 2yy_{i+1} - 2d_i d_{i+1} cos(\gamma_{i,i+1}), \qquad i = 1,2,\dots,M. \tag{4-23}$$

$$c_{i,i+1}^2 = 2R^2 + \left(x_i^2 + x_{i+1}^2 + y_i^2 + y_{i+1}^2\right) - 2x(x_i + x_{i+1}) - 2y(y_i + y_{i+1}) - 2d_i d_{i+1} cos(\gamma_{i,i+1}), \qquad i = 1,2,\dots,M, \tag{4-24}$$

where $R^2 = x^2 + y^2$. The purpose of these manipulations is to find a familiar form from earlier chapters. Rearranging (4-24),

$$x(x_i + x_{i+1}) + y(y_i + y_{i+1}) = R^2 + 0.5\left(x_i^2 + x_{i+1}^2 + y_i^2 + y_{i+1}^2\right) - d_i d_{i+1} cos(\gamma_{i,i+1}) - \frac{c_{i,i+1}^2}{2}, \qquad i = 1,2,\dots,M. \tag{4-25}$$

Equation (4-25) is the matrix-vector form like $\boldsymbol{A\theta} = \boldsymbol{b}$ in chapter 2,, where $\boldsymbol{\theta}$ is a vector consisting of unknown node coordinates ($\boldsymbol{\theta} = [x \quad y \quad R^2]^T$), and $\boldsymbol{A}$ and $\boldsymbol{b}$ matrices are:

$$\boldsymbol{A}_{M-1\times 3} = \begin{bmatrix} x_1 + x_2 & y_1 + y_2 & -1 \\ \vdots & \vdots & \vdots \\ x_{M-1} + x_M & y_{M-1} + y_M & -1 \end{bmatrix},$$

$$\boldsymbol{b}_{M-1\times 1} = \frac{1}{2}\begin{bmatrix} 0.5(x_1^2 + x_2^2 + y_1^2 + y_2^2 - c_1^2) - d_1 d_2 cos(\gamma_{1,2}) \\ \vdots \\ 0.5(x_{M-1}^2 + x_M^2 + y_{M-1}^2 + y_M^2 - c_M^2) - d_{M-1} d_M cos(\gamma_{M-1,M}) \end{bmatrix}. \tag{4-26}$$

The advantage of this hybrid technique compared to DAOA is that no specific layout of the anchors is required, i.e., it means that there is no need to have the anchors specifically on a circle around the unknown node for a closed form solution.

An unconstrained LS estimator is used now to estimate the unknown node position. This estimator ($\hat{\boldsymbol{\theta}} = (\boldsymbol{A}^T\boldsymbol{A})^{-1}\boldsymbol{A}^T\,\boldsymbol{b}$) is the same as that used in the previous chapters. The simulation result for the hybrid technique is shown in Figure 4-3. It is compared against the TOA technique which was used in chapter 2. The reason that the DAOA is not included in this comparison is that its anchor nodes do not have the same constellation as the other two algorithms (TOA and proposed hybrid TOA/DAOA). Fair comparison is only possible with identical anchor constellations. The simulations are undertaken for 10^4 observations and the results are averaged. Distance noise variance is the same as it was for TOA (0.1), and the angle noise variance is 2 degrees^2.

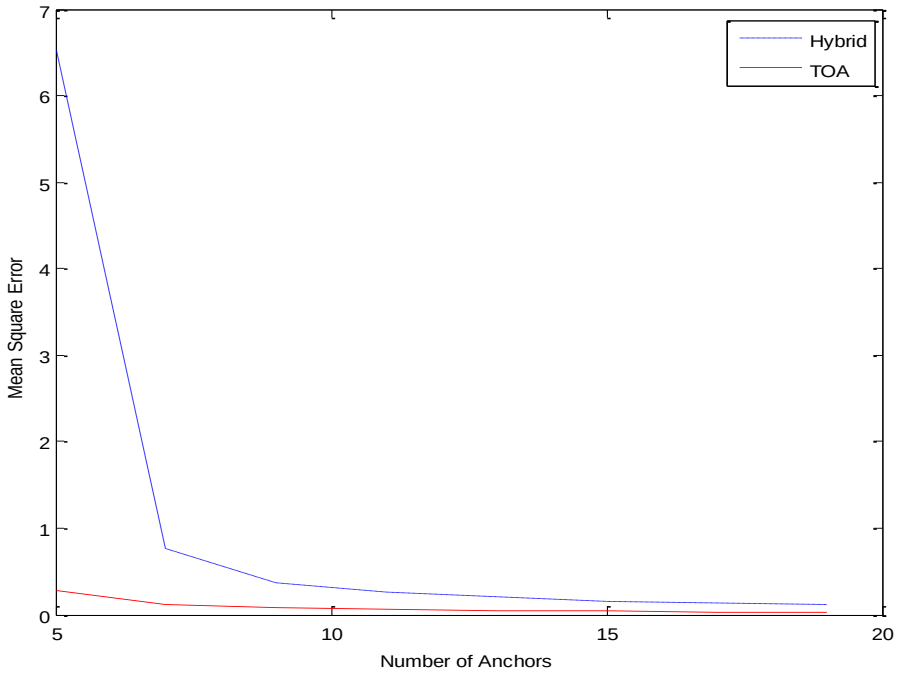

Figure 4-3. MSE vs. number of anchors in hybrid TOA/DAOA comparing to TOA. Distance noise variance=0.1, and angle variance=2 degrees^2.

The figure shows that the purely TOA technique has better performance than the hybrid. But any extra measurements, here the angle measurements, should improve the hybrid technique according estimation principles. The current algorithm – the LS - does not account for the different noise variances of the different (TOA and DAOA) measurements. The above figure is for the LS estimator which does not have prior

knowledge of the noise (noise covariance matrix), and this is why the results for the hybrid technique are less accurate than those for the purely TOA technique.

Having essentially noiseless angle measurements (very low angular noise variance) is not out of reach these days because of laser techniques. When the angle noise is zero, the proposed hybrid TOA/DAOA has a slightly better result than TOA technique for using more than eight anchors, as illustrated in Figure 4-4.

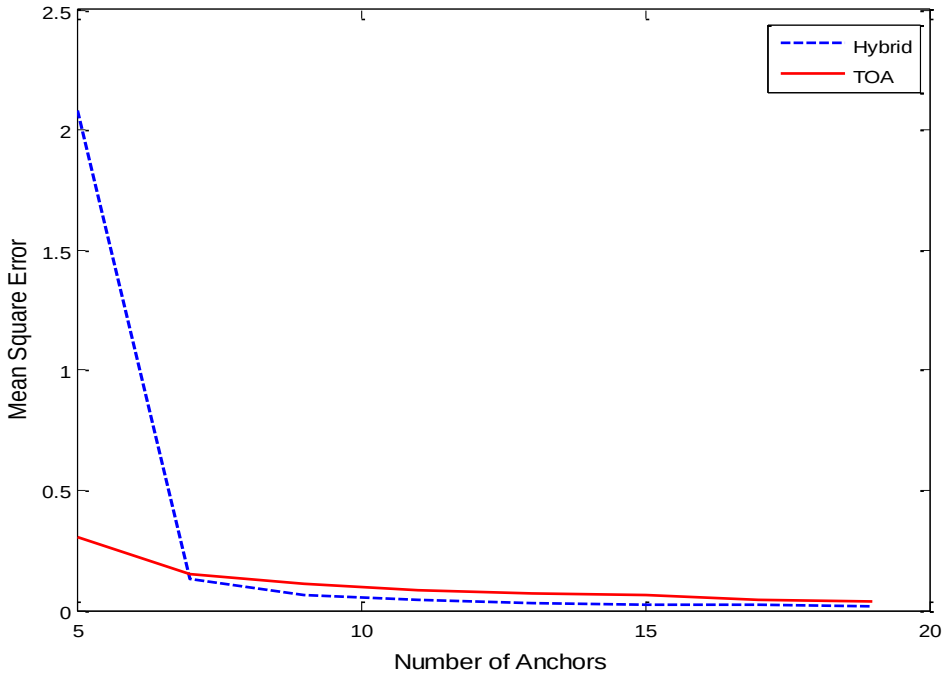

Figure 4-4. MSE vs. number of anchors in hybrid TOA/DAOA comparing to TOA. DNR=41, distance noise variance=0.1, and angle variance=0.

The results are presented here are to assist with future work for the case when the noise covariance is known. (Here the noise variance is known for the numerical experiments of the simulations, but it is not assumed to be known in the estimator, and this is also the case used in the cited literature.)

4.4. Considering the Localization Problem in Three-Dimensions

So far the localization problem is described in 2D. Positioning in 3D is also demanding. In this section 3D localization is briefly reviewed. The localization algorithm is the same as previous chapters except adding the third dimension to the calculations of the linear LS estimation algorithm. Figure 4-5 shows the notation for the position of the anchors and the unlocalized node in 3D. Here, (x, y, z) is the unknown node's coordinates, while (x_i, y_i, z_i) is the known coordinates of the i-th anchor. ϕ_i and α_i denote the azimuth and zenith angles, respectively. In the other words, ϕ_i is the azimuth angle of the projection of the unknown node on the $x-y$ plane, and α_i is the zenith angle of the unlocalized node. They can be shown as

$$\phi_i = tan^{-1}\left(\frac{y-y_i}{x-x_i}\right), \qquad \alpha_i = cos^{-1}\left(\frac{z-z_i}{d_i}\right), \tag{4-27}$$

where d_i is the distance between the unknown node and the i-th anchor. The calculation for d_i is similar to the 2D case in (2-7):

$$d_i = \sqrt{(x-x_i)^2 + (y-y_i)^2 + (z-z_i)^2}, \quad i = 1, 2, \ldots, M. \tag{4-28}$$

In the presence of noise, the distance and angles measurements become [12]

$$\hat{d}_i = d_i + n_{\hat{d}_i}, \qquad \hat{\varphi}_i = \varphi_i + n_{\hat{\varphi}_i}, \qquad \hat{\alpha}_i = \alpha_i + n_{\hat{\alpha}_i}; \tag{4-29}$$

where $n_{\hat{d}_i}$,$n_{\hat{\varphi}_i}$ and $n_{\hat{\alpha}_i}$ are the measurement errors of d_i,φ_i, and α_i respectively.

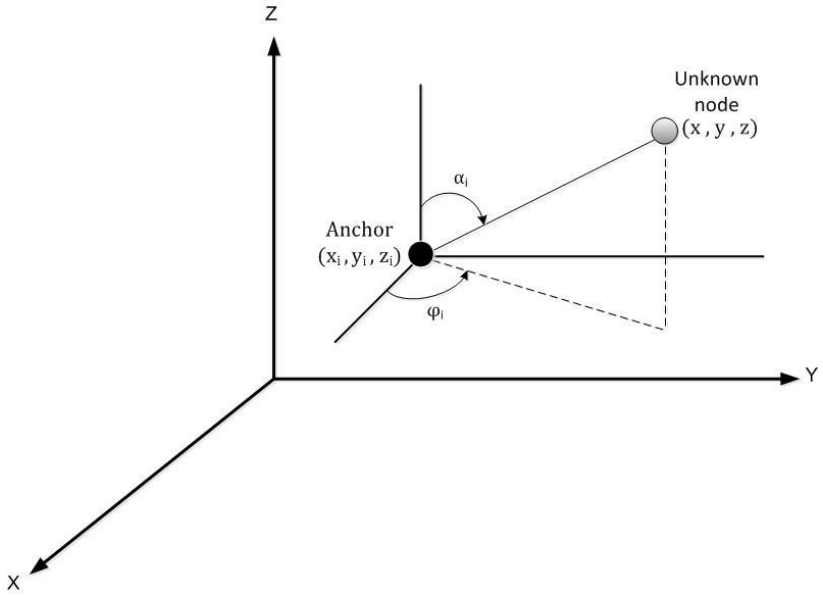

Figure 4-5. Representation of an unknown node and the anchor positions in 3D space.

4.4.1. Linear LS Method

Recalling from the previous chapters, the estimator for positioning the unlocalized node is LS. In order to develop this algorithm for the 3D case, only distance information is considered first. Then, the estimation algorithm is derived for the hybrid measurements when both the distance and angle measurements are available.

Estimation Based on Distance Measurements

Equation (4-28) has a nonlinear form, so in order to apply the LS estimator using only distances information, the equations are linearized. Squaring both sides of (4-28) and considering low noise in distances yields [12]

$$(x - x_i)^2 + (y - y_i)^2 + (z - z_i)^2 \approx \hat{d}_i^{\,2}, \;\; i = 1,2,\dots,M. \tag{4-30}$$

In order to produce a familiar form of the matrix-vector, the first anchor is taken as a reference node. Now a new element is introduced as follow [12]:

$$g_{i,1} \approx (x_i - x_1)x + (y_i - y_1)y + (z_i - z_1)z, \quad i = 2,3,\dots,M. \tag{4-31}$$

where $g_{i,1}$ is:

$$g_{i,1} = 0.5\left[(x_i{}^2 + y_i{}^2 + z_i{}^2) - (x_1{}^2 + y_1{}^2 + z_1{}^2) + \hat{d}_1^2 - \hat{d}_i^2\right]. \tag{4-32}$$

Equation (4-31) can be written in a matrix-vector form as:

$$\boldsymbol{M\beta} \approx \boldsymbol{g}, \tag{4-33}$$

where

$$\boldsymbol{M} = \begin{bmatrix} x_2 - x_1 & y_2 - y_1 & z_2 - z_1 \\ \vdots & \vdots & \vdots \\ x_M - x_1 & y_M - y_1 & z_M - z_1 \end{bmatrix}, \quad \boldsymbol{\beta} = \begin{bmatrix} x \\ y \\ z \end{bmatrix}, \quad \boldsymbol{g} = \begin{bmatrix} g_{2,1} \\ \vdots \\ g_{M,1} \end{bmatrix}. \tag{4-34}$$

Now the linear LS estimator is used to define the estimate of the position of the unknown node. It minimizes the sum of the squares of the difference between the two sides of each equation in (4-31). That is, [12]

$$\widehat{\boldsymbol{\beta}} = arg\,min_{\boldsymbol{\beta}} \sum_{i=2}^{M} w_{i-1}((x_i - x_1)x + (y_i - y_1)y + (z_i - z_1)z - g_{i,1})^2, \tag{4-35}$$

where $\{w_i\}$ are the weights which emphasize different elements of the measurements. The weighting concept is giving larger weights to the parameter measurements which are more reliable. For example, larger weights are assigned to the parameters of the anchors with a higher received signal power (the higher signal-to-noise). In some cases when *a priori* information on the distance estimation is not available, the weights may be chosen to be unity. The weighted LS (WLS) solution to (4-33) is given by

$$\widehat{\boldsymbol{\beta}} = (\boldsymbol{M}^T\boldsymbol{W}\boldsymbol{M})^{-1}\boldsymbol{M}^T\boldsymbol{W}\boldsymbol{g}, \tag{4-36}$$

where $\boldsymbol{M}$ should be full column rank (i.e., three in this case), to have a inverse matrix and the diagonal weighting matrix is

$$\boldsymbol{W}_{(M-1)\times(M-1)} = diag\{w_1, w_2, \dots, w_{M-1}\}, \tag{4-37}$$

Hybrid Estimation Based on Distance and Angle Measurements

When both distance and angle measurements are available, equations (4-27) and (4-28) change to [12]:

$$\begin{gathered} x \approx x_i + \hat{d}_i sin\hat{\alpha}_i cos\hat{\phi}_i, \quad y \approx y_i + \hat{d}_i sin\hat{\alpha}_i sin\hat{\phi}_i, \\ z \approx z_i + \hat{d}_i cos\hat{\alpha}_i, \quad i = 1,2, \dots, M. \end{gathered} \tag{4-38}$$

where the approximation is for the high SNR case. The interesting point when both the distance and angle measurements are available is that the unknown node can be localized by using only one anchor. When the LS estimation is applied to localize the unknown node's coordinate, the same form as (4-36) can be used, but with the following matrices [12]:

$$\begin{gathered} \boldsymbol{M}_{3M\times 3} = diag\{\mathbf{1}_M, \mathbf{1}_M, \mathbf{1}_M\}, \\ \boldsymbol{W}_{3M\times 3M} = diag\{w_1, w_1, \dots, w_{3M}\}, \\ \boldsymbol{g}_{3M\times 1} = [x_1 + \hat{d}_1 sin\hat{\alpha}_1 cos\hat{\phi}_1, \dots, x_M + \hat{d}_M sin\hat{\alpha}_M cos\hat{\phi}_M, \\ y_1 + \hat{d}_1 sin\hat{\alpha}_1 sin\hat{\phi}_1, \dots, y_M + \hat{d}_M sin\hat{\alpha}_M sin\hat{\phi}_M, \\ z_1 + \hat{d}_1 cos\hat{\alpha}_1, \dots., z_M + \hat{d}_M cos\hat{\alpha}_M \ ]^T. \end{gathered} \tag{4-39}$$

4.5. Conclusions

In this chapter, the hybrid TDOA/AOA was reviewed. The same LS approach as previous algorithms discussed in chapters 2 and 3 is used. This hybrid technique is considered in the literature as a better algorithm with higher accuracy for localization. However, the goal of this thesis was to use an algorithm using TOA/DAOA as the measurements. This new proposed hybrid localization algorithm was undertaken in a similar manner of previously discussed algorithms.

The simulation result for the proposed TOA/DAOA technique was compared to the unconstrained TOA technique obtained in chapter 2. The noise variance of the distance measurements were the same (0.1) for both techniques. DAOA noise in this hybrid algorithm was 2 degrees^2. With this level of angle noise, the performance of the hybrid could not beat the TOA method. However, for the second comparison, the angle noise was set to zero and the result showed the slightly better performance for hybrid algorithm than the TOA algorithm.

Chapter 5: Conclusions and Future Work

5.1. Summary and Conclusions

Accurately positioning an unknown node in a wireless sensor network is very difficult. All the nodes are equipped with the transmitters and receivers to communicate between each other. Based on the positioning application, this problem can be categorized. One category is range-based localization in a static sensor network, and this is the subject of this thesis. Various measurement techniques (such as RSS, TOA, TDOA, AOA, hybrid TDOA/AOA) have been proposed and discussed in the literature. The focus here was on TOA, AOA, DAOA and hybrid TOA/DAOA.

In chapter 2, the focus was on localization algorithms using TOA measurements. A new nonlinear estimation method was presented in order to apply to a one-dimensional network topology. This estimator had a good performance compared to the derived Cramer-Rao bound. The nonlinear least squares estimator was presented in order to use for two-dimension case as well. The simulation results were presented graphically as useful design information. A Distance-to-Noise-Ratio (DNR) was introduced as a parameter in chapter 2 in order to evaluate the performance of the estimators. DNR is the ratio between the squared mean of the distance, u_d^2, and the noise variance, σ_n^2, and it calculated from $10\log\frac{u_d^2}{\sigma_n^2}$. So, this is the obvious analogy of SNR as used in other signal processing disciplines. Also in chapter 2, the nonlinear equations were reorganized into a set of linear equations in order to reduce the complexity (of NLSE). The constrained and unconstrained Least Squares (ULS) location algorithm using TOA measurements were reviewed. The simulation results for ULS were essentially the same as those of NLSE, and the weighted ULS having a slightly lower MSE.

In chapter 3, angular measurements of the nodes were considered for the localization algorithms. The unconstrained and weighted unconstrained least squares location algorithms using absolute AOA are also reviewed. A goal of this thesis was to develop a localization algorithm which considers the angles between the anchors and the unlocalized node, i.e., the Differential-Angle-of-Arrival. This was a new measurement technique developed in this thesis motivated by using rotating lasers. Triangulation (cosine law) was used to calculate the distances between nodes. For simplicity in the simulations, the anchors were confined to being on a circle around the unlocalized node, and LS estimation was used for the unlocalized node location. Simulations showed that using more than 8 anchors had reached diminishing returns.

In chapter 4, localization algorithms using hybrid technique were investigated. A short review on TDOA measurement was provided. In addition, TOA and DAOA techniques from the previous chapters were incorporated to develop a new hybrid technique. Least Squares was used for the estimation of the unknown node. The simulations for the proposed TOA/DAOA technique were compared to unconstrained TOA technique obtained in chapter 2. With the chosen simulation noise variances (0.1 for the distance noise variance, and 2 degrees^2 for the DAOA noise variance) the LS estimator used in the hybrid method could not beat the LS estimator that used purely TOA. With zero angular noise, the hybrid algorithm was essentially the same as the pure TOA for more than 8 anchors.

5.2. Future Work

Throughout this thesis, LOS signal propagation was assumed in a static sensor network consisting of for example, 10 to 20 anchors. There was one unlocalized node among these anchors. There were also two other assumptions throughout this thesis. In chapter 2, the distances between the anchors and the unlocalized node were given with a certain noise variance. In chapter 3, the angle subtending two anchors from the unlocalized node was known with a certain noise variance. For the hybrid algorithm, both noises were considered. So, this thesis did not deal with the real experimental measurements and the presented results were all based on the simulations. With these assumptions in mind, the following directions beckon:

- **Considering NLOS signal propagations:**

  LOS propagation is not always available in the systems. Due to reflections and diffractions of the signals, one of the major error sources in mobile location is NLOS error propagation. It degrades the localization or tracking accuracy significantly. Therefore, algorithms which could discard the NLOS measurements or formulate the positioning and tracking problem with NLOS are required. Positioning with NLOS propagations is a major challenge, and is a fertile area for more research.

- **Knowing the exact coordinates of just a few number of anchors and calculate the other anchors positions:**

  In some situations the exact coordinates of some of the anchors is not available. Finding these anchors' coordinates from the known coordinates of the other anchors is a good direction for future work. Also, Investigation of anchor-free localization schemes remains a major challenge, e.g. [25].

- **Considering DAOA for generalized constellations of anchors:**

  The DAOA simulations were confined to a specific, circular configuration for simplicity. The obvious extension here is to generalize this layout and determine the sensitivity to the geometric situation.

- **Extension of the localization algorithms for estimating of more than one unlocalized node:**

  Localization of one static node can be used iteratively in order to locate more unknown nodes. Whenever an unknown node is localized, it can be considered as a new anchor for the system and helps to improve the accuracy of localizing other unknown nodes. Such iterative schemes can be an extension to this research.

- **Extension of the localization algorithms for estimating of a mobile unlocalized node:**

  The unknown node was static in this thesis. However, localizing a mobile station is an interesting problem. Positioning a mobile target (tracking) is another extension to this research. A trajectory can be determined and different algorithm can be applied for the localization. Kalman filtering has been a traditional choice, but the sensitivity to the non-gaussian noise compromises this approach.

- **Extension of the localization algorithms for N dimensional localization:** N-dimensional location where N is greater than the usual cartesian coordinates is possible in a mathematical sense. This type of calculation is not applicable to physical situations, but may have applications in multi-dimensional systems such as data bases.

References

[1] M. Rudafshani and S. Datta, “Localization in wireless sensor networks,” *Information Processing in Sensor Networks (IPSN)*, 2007.

[2] J. Bachrach and C. Taylor, *Handbook of Sensor Networks: Algorithms and Architectures, I. Stojmenovic, Ed., Wiley,* Sept. 2005.

[3] H. Liu, H. Darabi, P. Banerjee, and J. Liu, “Survey of wireless indoor positioning techniques and systems,” *IEEE Trans. Syst., Man, Cybern. C: Applications and Reviews,* vol. 37, no. 6, 2007.

[4] Z. Sahinoglu, S. Gezici, and I. Guvenc, *Ultra-wideband Positioning Systems, Cambridge University Press*, 2008.

[5] G. Mao and B. Fidan, *Localization Algorithms and Strategies for Wireless Sensor Networks, IGI Global*, 2009.

[6] R. Stoleru, T. He, J.A. Stankovic, D. Luebke, “A high-accuracy, low-cost localization system for wireless sensor networks,” *Proceedings of the Third International Conference on Embedded Networked Sensor Systems (Sensys), San Diego, CA*, 2005.

[7] K.W. Cheung, M.C. So, W.-K. Ma, Y.T. Chan, “A constrained least squares approach to mobile positioning: algorithms and optimality,” *EURASIP J. Appl. Signal Process,* 2006.

[8] H. Tang, Y. Park, and T. Qiu, “A TOA-AOA-based NLOS error mitigation method for location estimation,” *EURASIP J. Adv. Signal Process,* vol. 8, no. 1, 2008.

[9] K. Yu, Y.J. Guo, M. Hedley, “TOA-based distributed localization with unknown internal delays and clock frequency offsets in wireless sensor networks,” *IET Signal Process*, 2009, 51.

[10] R. Peng and M. L. Sichitiu, “Angle of Arrival Localization for Wireless Sensor Networks,” *Proc. Conf. Sensor and Ad-Hoc Comm. and Networks*, 2006.

[11] A.Pagès-Zamora, J. Vidal Manzano, and D.H. Brooks, “Closed-form solution for positioning based on angle of arrival measurements,” *Proc. 13th IEEE Int. Symp. Personal, Indoor and Mobile Radio Communications, Lisbon, Portugal,* Sep. 2002.

[12] K. Yu, “3D localization error analysis in wireless networks,” *IEEE Trans.Wireless Commun.*, vol. 6, no. 10, Oct. 2007.

[13] K. Almuzaini, *Time Synchronization and Localization in Wireless Networks, PhD dissertation*.

[14] Rodney G. Vaughan, “Compact Multiport Antennas for High Spectral Efficiency Motivation from Energy Considerations, Lessons from Early Wireless History, and Design," European Conference on Antennas and Propagation (Eucap 2013), Gothenburg, Sweden, April 2013.

[15] F. Liu, X. Cheng, D. Hua, and D. Chen, “*TPSS: a timebased positioning scheme for sensor networks with short range beacons,” Wireless Sensor Networks and Applications*, pp. 175–193, Springer, New York, NY, USA, 2008.

[16] P. Kułakowski, J. Vales-Alons, E. Egea-Lopez, W. Ludwin, J. Garcia-Haro, “Angle-of-arrival localization based on antenna arrays for wireless sensor networks,” *Elsevier computers and electrical engineering journal,* vol.36(6); 2010. pp. 1181–6.

[17] M. Boushaba, A. Hafid, A. Benslimane, “High accuracy localization method using AoA in sensor networks,” *Computer Networks* 53, 3087–3088, 2009.

[18] G. Sun, J. Chen, W. Guo, and K.J.R. Liu, “Signal processing techniques in network-aided positioning,” *IEEE Signal Processing Mag.,* vol. 22, no. 4, pp. 12–23, July 2005

[19] A. Baggio, K. Langendoen, “Monte Carlo localization for mobile wireless sensor networks,” *Ad Hoc Networks,* no. 6, pp. 718–733, 2008.

[20] J. Wang, R.K. Ghosh, and S. Daskin, “A survey on sensor localization,” *Journal of Control Theory and Applications,* 8(1): 2–11, 2010.

[21] F. Franceschini, M. Galetto, D. Maisano, and L. Mastrogiacomo “A Review of Localization Algorithms for Distributed Wireless Sensor Networks in Manufacturing,” *International Journal of Computer Integrated Manufacturing,* vol. 1, no. 1, pp. 1–19, 2007.

[22] A.N. Bishop, B. Fidan, K. Dogancay, B.D.O. Anderson, and P.N. Pathirana, “*Exploiting geometry for improved hybrid AOA/TDOA based localization,*” Signal Processing, 88(7):1775–1791, July 2008.

[23] L. Cong and W. Zhuang, “Hybrid, TDOA/AOA mobile user location for wide-band CDMA cellular systems,” *IEEE Trans. Wireless Commun.*, vol. 1, no. 3, pp. 439–447, July 2002.

[24] S. A. Banani, M. Najibi, and R.G. Vaughan, “Range-based Localisation and tracking in NLOS Wireless Channels with GSDM,” *IET Signal Process*, submitted May 2012, currently under revision.

[25] K. Yu and Y. J. Guo, “Anchor-free localization algorithm and performance analysis in wireless sensor networks,” *IET Commun.*, Mar. 2008.

[26] R. Stoleru, J.A. Stankovic, “Probability grid: a location estimation scheme for wireless sensor networks,” *IEEE SECON*, 2004.

[27] J. Arias, J. Ĺazaro, A. Zuloaga, J. Jiḿenez, and A. Astarloa, “GPS-less location algorithm for wireless sensor networks,” *Computer Communications*, vol. 30, no. 14-15, pp. 2904–2916, 2007.

[28] G. Mao, B. Fidan, B.D.O. Anderson, “Wireless sensor network localization techniques,” *Elsevier/ACM Computer Networks* 51 (10), pp. 2529–2553, 2007.

[29] K.W. Cheung, H.C. So, W.K. Ma, and Y.T. Chan, “Least squares algorithms for time-of-arrival-based mobile location,” *IEEE Trans. Signal Processing*, vol. 52, no.4, pp. 1121–1130, Apr. 2004.

[30] J. 0. Smith and J. S. Abel, “Closed-form least-squares source location estimation from range-difference measurements,” *IEEE Trans. Acoust., Speech, Signal Processing*, vol. ASSP-35, pp. 1661-1669.

[31] M.L. Sichitiu and V. Ramadurai, “Localization of wireless sensor networks with a mobile beacon,” *Center for Advances in Computing and Communication (CACC),* Raleigh, NC, Tech. Rep. TR-03/06, July 2003.

[32] A. Boukerche, H. Oliveira, E. Nakamura, and A. Loureiro, “Localization systems for wireless sensor networks,” *IEEE Wireless Commun. Mag.*, vol. 14, no. 6, pp. 6–12, Dec. 2007

[33] L. Cong, W. Zhuang, “Non-line-of-sight error mitigation in TDOA mobile location,” *IEEE Global Telecommunications Conference, GLOBECOM ’01,* vol. 1, 2001, pp. 680–684.

[34] W. Yang, “Source localization using TDOA measurements with sensor Location Uncertainty,” *30th Chinese Control Conference*, Yantai, China, July 2011.

[35] W. Wang, Q. Zhu, “High accuracy geometric localization scheme for wireless sensor networks,” International Conference on Communications, Circuits and Systems (ICCCAS), Vol. 3, pp. 1507–1512, 2006.

[36] C. Saad, A. Benslimane, and J.-C. Konig, “At-angle: A distributed method for localization using angles in sensor networks,” *Computers and Communications, 2008. ISCC 2008. IEEE Symposium,* pp. 1190–1195, July 2008.

Appendices

Appendix A.

Mathematical Calculations of NLSE

In one-dimension localization, expanding the cost function (J) in equation (2-17) is as follows:

$$J = \sum_{i=1}^{M} ((x - x_i)^4 + d_i^4 - 2(x - x_i)^2 d_i^2) \,. \tag{A.1}$$

$$J = \sum_{i=1}^{M} (x^2 + x_i^2 - 2xx_i)^2 + \sum_{i=1}^{M} d_i^4 - 2\sum_{i=1}^{M} (xd_i - x_i d_i)^2 \,. \tag{A.2}$$

For convenience, the summations can be considered as multiplications of two vectors. So, the following vectors are introduced here to use in the calculations:

$$D = \begin{bmatrix} d_1 \\ \vdots \\ d_M \end{bmatrix}, \boldsymbol{v} = \begin{bmatrix} x_1 \\ \vdots \\ x_M \end{bmatrix}, \boldsymbol{w} = \begin{bmatrix} y_1 \\ \vdots \\ y_M \end{bmatrix}, \boldsymbol{p} = \begin{bmatrix} x_1^2 \\ \vdots \\ x_M^2 \end{bmatrix}, \boldsymbol{q} = \begin{bmatrix} y_1^2 \\ \vdots \\ y_M^2 \end{bmatrix}, \mathbf{1}_{\mathrm{M}} = \begin{bmatrix} 1 \\ \vdots \\ 1 \end{bmatrix}. \tag{A.3}$$

In terms of multiplications, (A.2) changes to

$$\begin{aligned} J \;=\; & \|x^2 1 + \boldsymbol{p} - 2x\boldsymbol{v}\|^T \|x^2 1 + \boldsymbol{p} - 2x\boldsymbol{v}\| + \sum_{i=1}^{M} d_i^4 \\ & - 2\|xD - \boldsymbol{v} \odot D\|^T \|xD - \boldsymbol{v} \odot D\| \end{aligned} \tag{A.4}$$

$$\begin{aligned} = Mx^4 + \boldsymbol{p}^T\boldsymbol{p} + 4x^2\boldsymbol{v}^T\boldsymbol{v} + 2x^2\mathbf{1}_M^T\boldsymbol{p} - 4x^3\mathbf{1}_M^T\boldsymbol{v} - 4x\boldsymbol{p}^T\boldsymbol{v} + \sum_{i=1}^{M} d_i^4 - \\ 2(x^2 D^T D + (\boldsymbol{v} \odot D)^T(\boldsymbol{v} \odot D) - 2xD^T(\boldsymbol{v} \odot D)) \end{aligned} \tag{A.5}$$

$$\begin{aligned} = \; Mx^4 + \boldsymbol{p}^T p + 4x^2\boldsymbol{v}^T\boldsymbol{v} + 2x^2\mathbf{1}_M^T\boldsymbol{p} - 4x^3\mathbf{1}_M^T\boldsymbol{v} - 4x\boldsymbol{p}^T\boldsymbol{v} + \sum_{i=1}^{M} d_i^4 - 2x^2 D^T D \\ - 2(\boldsymbol{v} \odot D)^T(\boldsymbol{v} \odot D) + 4xD^T(\boldsymbol{v} \odot D), \end{aligned} \tag{A.6}$$

where $\odot$ means the inner product of corresponding elements of two vectors. So, the derivative of J with respect to x would be:

$$\begin{aligned}\frac{\partial J}{\partial x} &= 4Mx^3 + 8x\boldsymbol{v}^T\boldsymbol{v} + 4x\mathbf{1}_M^T\boldsymbol{p} - 12x^2\mathbf{1}_M^T\boldsymbol{v} - 4\boldsymbol{p}^T\boldsymbol{v} - 4xD^TD + 4D^T(\boldsymbol{v}\odot D)\\ &= Mx^3 - 3x^2(\mathbf{1}_M^T\boldsymbol{v}) + x(2\boldsymbol{v}^T\boldsymbol{v} + \mathbf{1}_M^T\boldsymbol{p} - D^TD) + D^T(\boldsymbol{v}\odot D) - \boldsymbol{p}^T\boldsymbol{v}\,.\end{aligned} \tag{A.7}$$

Since the cost function must be minimized, this derivative is set to zero. The real root of this cubic equation is:

$$x = \frac{3(\mathbf{1}_M^T\boldsymbol{v})}{3M} - \frac{2^{1/3}\left(-(-3(\mathbf{1}_M^T\boldsymbol{v}))^2 + 3M(2\boldsymbol{v}^T\boldsymbol{v} + 1^T\boldsymbol{p} - D^TD)\right)}{3M\boldsymbol{u}} + \frac{\boldsymbol{u}}{3\times 2^{1/3}M}\,, \tag{A.8}$$

where $\boldsymbol{u}$ equals:

$$\begin{aligned}[-2(-3(\mathbf{1}_M^T\boldsymbol{v}))^3 &+ 9M(-3(\mathbf{1}_M^T\boldsymbol{v})(2\boldsymbol{v}^T\boldsymbol{v} + \mathbf{1}_M^T\boldsymbol{p} - D^TD) - 27M^2(D^T(\boldsymbol{v}\odot D) - \boldsymbol{p}^T\boldsymbol{v})\\ &+ (\,4\{-(-3(\mathbf{1}_M^T\boldsymbol{v}))^2 + 3M(2\boldsymbol{v}^T\boldsymbol{v} + \mathbf{1}_M^T\boldsymbol{p} - D^TD)\}^3\\ &+ \{-2(-3(\mathbf{1}_M^T\boldsymbol{v}))^3 + 9M(-3(\mathbf{1}_M^T\boldsymbol{v}))(2\boldsymbol{v}^T\boldsymbol{v} + \mathbf{1}_M^T\boldsymbol{p} - D^TD)\\ &- 27M^2(D^T(\boldsymbol{v}\odot D) - \boldsymbol{p}^T\boldsymbol{v})\}^2)^{\frac{1}{2}}\,]^{\frac{1}{3}}\,.\end{aligned} \tag{A.9}$$

In two-dimension localization, expanding the cost function (J) in equation (2-20) is as follows:

$$\begin{aligned}J = \sum_{i=1}^{M}[&(x-x_i)^4 + (y-y_i)^4 + 2(x-x_i)^2(y-y_i)^2 + d_i^4 - 2d_i^2(x-x_i)^2\\ &- 2d_i^2(y-y_i)^2]\end{aligned} \tag{A.10}$$

$$\begin{aligned}= \sum_{i=1}^{M}(x^2 + x_i^2 - 2xx_i)^2 + \sum_{i=1}^{M}(y^2 + y_i^2 - 2yy_i)^2 + 2\sum_{i=1}^{M}(x-x_i)^2(y-y_i)^2 + \sum_{i=1}^{M}d_i^4\\ - 2\sum_{i=1}^{M}d_i^2(x-x_i)^2 - 2\sum_{i=1}^{M}d_i^2(y-y_i)^2\end{aligned} \tag{A.11}$$

$$= \sum_{i=1}^{M}(x^2 + x_i^2 - 2xx_i)^2 + \sum_{i=1}^{M}(y^2 + y_i^2 - 2yy_i)^2 + 2\sum_{i=1}^{M}(xy - xy_i - yx_i + x_iy_i)^2 + \sum_{i=1}^{M} d_i^4 - 2\sum_{i=1}^{M}(xd_i - x_id_i)^2 - 2\sum_{i=1}^{M}(yd_i - y_id_i)^2 \quad \text{(A.12)}$$

$$= \|x^2\mathbf{1}_{\mathrm{M}} + \boldsymbol{p} - 2x\boldsymbol{v}\|^T\|x^2\mathbf{1}_{\mathrm{M}} + \boldsymbol{p} - 2x\boldsymbol{v}\| + \|y^2\mathbf{1}_{\mathrm{M}} + \boldsymbol{q} - 2y\boldsymbol{w}\|^T\|y^2\mathbf{1}_{\mathrm{M}} + \boldsymbol{q} - 2y\boldsymbol{w}\| + \sum_{i=1}^{M} d_i^4 + 2\|xy\mathbf{1}_{\mathrm{M}} - x\boldsymbol{w} - y\boldsymbol{v} + \boldsymbol{v}\odot\boldsymbol{w}\|^T\|xy\mathbf{1}_{\mathrm{M}} - x\boldsymbol{w} - y\boldsymbol{v} + \boldsymbol{v}\odot\boldsymbol{w}\| - 2\|Dx - D\odot\boldsymbol{v}\|^T\|Dx - D\odot\boldsymbol{v}\| - 2\|Dy - D\odot\boldsymbol{w}\|^T\|Dy - D\odot\boldsymbol{w}\| \quad \text{(A.13)}$$

$$= Mx^4 + \boldsymbol{p}^T\boldsymbol{p} + 4x^2\boldsymbol{v}^T\boldsymbol{v} + 2x^2\mathbf{1}_M^T\boldsymbol{p} - 4x^3\mathbf{1}_M^Tv - 4x\boldsymbol{p}^T\boldsymbol{v} + My^4 + \boldsymbol{q}^T\boldsymbol{q} + 4y^2\boldsymbol{w}^T\boldsymbol{w} + 2y^2\mathbf{1}_M^T\boldsymbol{q} - 4y^3\mathbf{1}_M^T\boldsymbol{w} - 4y\boldsymbol{q}^T\boldsymbol{w} + \sum_{i=1}^{M} d_i^4 + 2\big(Mx^2y^2 + x^2\boldsymbol{w}^T\boldsymbol{w} + y^2v^T\boldsymbol{v} + (\boldsymbol{v}\odot\boldsymbol{w})^T(\boldsymbol{v}\odot\boldsymbol{w}) - 2x^2y\mathbf{1}_M^T\boldsymbol{w} - 2xy^2\mathbf{1}_M^T\boldsymbol{v} + 2xy\mathbf{1}_M^T(\boldsymbol{v}\odot\boldsymbol{w}) + 2xy\boldsymbol{w}^T\boldsymbol{v} - 2x\boldsymbol{w}^T(\boldsymbol{v}\odot\boldsymbol{w}) - 2y\boldsymbol{v}^T(\boldsymbol{v}\odot\boldsymbol{w})\big) - 2\big(D^TDx^2 + (D\odot\boldsymbol{v})^T(D\odot\boldsymbol{v}) - 2D^Tx(D\odot\boldsymbol{v})\big) - 2\big(D^TDy^2 + (D\odot\boldsymbol{w})^T(D\odot\boldsymbol{w}) - 2D^Ty(D\odot\boldsymbol{w})\big). \quad \text{(A.14)}$$

Derivations of J with respect to x and y are:

$$\frac{\partial J}{\partial x} = 4Mx^3 + 8x\boldsymbol{v}^T\boldsymbol{v} + 4x\mathbf{1}_M^T\boldsymbol{p} - 12x^2\mathbf{1}_M^T\boldsymbol{v} - 4\boldsymbol{p}^T\boldsymbol{v} + 2\big(2Mxy^2 + 2x\boldsymbol{w}^T\boldsymbol{w} - 4xy\mathbf{1}_M^T\boldsymbol{w} - 2y^2\mathbf{1}_M^T\boldsymbol{v} + 2y\mathbf{1}_M^T(\boldsymbol{v}\odot\boldsymbol{w}) + 2y\boldsymbol{w}^T\boldsymbol{v} - 2\boldsymbol{w}^T(\boldsymbol{v}\odot\boldsymbol{w})\big) - 2\big(2xD^TD - 2D^T(D\odot\boldsymbol{v})\big) \quad \text{(A.15)}$$

$$= 2y^2\ (Mx - \ \mathbf{1}_M^T \boldsymbol{v}) + 2\ y\ (\mathbf{1}_M^T\ (\boldsymbol{v} \odot \boldsymbol{w}) - \ 2x\ \mathbf{1}_M^T\ \boldsymbol{w} + \ \boldsymbol{w}^T\ \boldsymbol{v}) + \ \boldsymbol{f}(x); \tag{A.16}$$

$$\begin{aligned}\frac{\partial J}{\partial y} = {} & 4My^3 + 8y\boldsymbol{w}^T\boldsymbol{w} + 4y\mathbf{1}_M^T\boldsymbol{q} - 12y^2\mathbf{1}_M^T\boldsymbol{w} - 4\boldsymbol{q}^T \\ & + 2\big(2Mx^2y + 2y\boldsymbol{v}^T\boldsymbol{v} - 4xy\mathbf{1}_M^T\boldsymbol{v} - 2x^2\mathbf{1}_M^T\boldsymbol{w} + 2x\mathbf{1}_M^T(\boldsymbol{v} \odot \boldsymbol{w}) \\ & + 2x\boldsymbol{w}^T\boldsymbol{v} - 2\boldsymbol{v}^T(\boldsymbol{v} \odot \boldsymbol{w})\big) - 2\big(2yD^TD - 2D^T(D \odot \boldsymbol{w})\big)\end{aligned} \tag{A.17}$$

$$= 2x^2\ (My - \ \mathbf{1}_M^T\boldsymbol{w}) + \ 2x\ (\mathbf{1}_M^T\ (\boldsymbol{v}\ \odot\ \boldsymbol{w}) - \ 2y\ \mathbf{1}_M^T\ \boldsymbol{v} + \ \boldsymbol{w}^T\ \boldsymbol{v}) + \ \boldsymbol{g}(y); \tag{A.18}$$

where $\boldsymbol{f}(x)$ and $\boldsymbol{g}(y)$ are as below:

$$\begin{aligned}\boldsymbol{f}(x) = {} & 2Mx^3 - \ 6\ x^2\ \mathbf{1}_M^T\ \boldsymbol{v} + 2x\ (2\ \boldsymbol{v}^T\ \boldsymbol{v} + \ \mathbf{1}_M^T\ \boldsymbol{p} + \ \boldsymbol{w}^T\ \boldsymbol{w} - \ D^T\ D) - \ 2\boldsymbol{p}^T\ \boldsymbol{v} \\ & - \ 2w^T\ (v \odot w) + \ 2D^T\ (D \odot v);\end{aligned} \tag{A.19}$$

$$\begin{aligned}\boldsymbol{g}(y) = {} & 2My^3 - \ 6\ y^2\ \mathbf{1}_M^T\ \boldsymbol{w} + 2y\ (2\ \boldsymbol{w}^T\ \boldsymbol{w} + \ \mathbf{1}_M^T\ \boldsymbol{q} + \ \boldsymbol{v}^T\ \boldsymbol{v} - \ D^T\ D) - \ 2\boldsymbol{q}^T\ \boldsymbol{w} \\ & - \ 2\boldsymbol{v}^T\ (\boldsymbol{v} \odot \boldsymbol{w}) + \ 2D^T\ (D \odot \boldsymbol{w}).\end{aligned} \tag{A.20}$$

Appendix B.

Calculation of CRLB for 1D Localization

From estimation theory, suppose θ is an unknown deterministic parameter which is to be estimated from measurements x with the conditional probability density function of $f(x|\theta)$. The variance of any unbiased estimator, $\hat{\theta}$, is then bounded by the inverse of the Fisher information function $I(\theta)$:

$$var_{\hat{\theta}}(\theta) \geq \frac{1}{I(\theta)}, \tag{B.1}$$

where

$$I(\theta) = E\left[\left(\frac{\partial ln\, P(\boldsymbol{x}\,|\theta)}{\partial\theta}\right)^2\right] = -E\left[\frac{\partial^2 ln\, P(\boldsymbol{x}|\theta)}{\partial\theta^2}\right]. \tag{B.2}$$

Now, $var_{\hat{\theta}}(\theta)$ needs to be determined for NLSE in 1D case. Suppose u_i as the distance measurement between unknown node and an anchor in 1D case:

$$u_i = |A - Z_i| + n_i\,, \tag{B.3}$$

where A is the coordinates of unknown node, Z_i is the anchor, and n_i the Gaussian noise. Distribution of u_i is the same as its noise:

$$f_u(u_i|\mathrm{A}) = \frac{1}{\sqrt{2\pi\sigma^2}}\exp\left\{\frac{-1}{2\sigma^2}(u_i - |A - Z_i|)^2\right\}. \tag{B.4}$$

where σ^2 is the noise variance. Then for M anchors the distribution would be:

$$f_u(\boldsymbol{u}|A) = \frac{1}{\sqrt{(2\pi\sigma^2)^M}}\exp\left\{\frac{-1}{2\sigma^2}\sum_{i=1}^{M}(u_i - |A - Z_i|)^2\right\}. \tag{B.5}$$

Knowing that $ln(ab) = ln(a) + ln(b)$, taking $ln(.)$ from both sides of (B.5) changes it to:

$$\ln f = \ln\left(\frac{1}{\sqrt{(2\pi\sigma^2)^M}}\right) - \frac{1}{2\sigma^2}\sum_{i=1}^{M}(u_i - |A - Z_i|)^2. \tag{B.6}$$

In order to obtain the Fisher information function, second derivative of (B.6) must be taken. Recalling $\frac{d}{du}|u| = \frac{u}{|u|}\,u'$, the first derivative of (B.6) with respect to A is:

$$\frac{\partial \ln f}{\partial A} = \frac{1}{\sigma^2}\sum_{i=1}^{M}(u_i - |A - Z_i|)\frac{(A - Z_i)}{|A - Z_i|} = \frac{1}{\sigma^2}\sum_{i=1}^{M}(\frac{u_i(A - Z_i)}{|A - Z_i|} - A + Z_i)\,. \tag{B.7}$$

By taking another derivate from (B.7) with respect to A, first and third terms would be zero:

$$\frac{\partial}{\partial A}\left(\sum_{i=1}^{M}\frac{u_i(A - Z_i)}{|A - Z_i|}\right) = \sum_{i=1}^{M}\frac{u_i|A - Z_i| - \frac{(A - Z_i)^2}{|A - Z_i|}}{(A - Z_i)^2} = 0,$$
$$\frac{\partial}{\partial A}\left(\sum_{\mathrm{i=1}}^{\mathrm{M}} Z_i\right) = 0\,. \tag{B.8}$$

So, $\frac{\partial^2 ln\, f}{\partial A^2}$ has the form

$$\frac{\partial^2 ln\, f}{\partial A^2} = \frac{1}{\sigma^2}\sum_{i=1}^{M}(-1) = \frac{-M}{\sigma^2}. \tag{B.9}$$

Now, as (B.2) shows the expectation of (B.9) has to be taken ($-E\left[\frac{\partial^2 ln\, f}{\partial A^2}\right] = -E\left[\frac{-M}{\sigma^2}\right]$). Then substituting it in (B.1) determines a bound for the variance of the estimation. So, $\frac{\sigma^2}{M}$ is considered as the CRLB in 1D case, where M is the number of known points or anchors and σ^2 is variance of the noise.